Check for updates

FEBS Letters

FEBS PRESS science publishing by scientists

REVIEW

Molecular analysis of the extracellular microenvironment: from form to function

Jade K. Macdonald, Anand S. Mehta, Richard R. Drake and Peggi M. Angel

Department of Cell and Molecular Pharmacology & Experimental Therapeutics, Medical University of South Carolina, Charleston, SC, USA

Correspondence
P. M. Angel, Department of Cell and Molecular Pharmacology & Experimental Therapeutics, Medical University of South Carolina, 173 Ashley Avenue BSB 358, Charleston, SC 29425, USA
Tel: +1 843 792-8410
E-mail: angelp@musc.edu

(Received 29 November 2023, revised 26 February 2024, accepted 28 February 2024, available online 21 March 2024)

doi:10.1002/1873-3468.14852

Edited by Lukas Alfons Huber

The extracellular matrix (ECM) proteome represents an important component of the tissue microenvironment that controls chemical flux and induces cell signaling through encoded structure. The analysis of the ECM represents an analytical challenge through high levels of post-translational modifications, protease-resistant structures, and crosslinked, insoluble proteins. This review provides a comprehensive overview of the analytical challenges involved in addressing the complexities of spatially profiling the extracellular matrix proteome. A synopsis of the process of synthesizing the ECM structure, detailing inherent chemical complexity, is included to present the scope of the analytical challenge. Current chromatographic and spatial techniques addressing these challenges are detailed. Capabilities for multimodal multiplexing with cellular populations are discussed with a perspective on developing a holistic view of disease processes that includes both the cellular and extracellular microenvironment.

Keywords: collagen; extracellular matrix; mass spectrometry imaging; matrisome; proteomics; spatial biology; spatial omics

The extracellular matrix (ECM) is a three-dimensional complex network with significant proteins and post-translational patterns that forms the tissue microenvironment (TME) outside of the cell. Far from being a bare scaffold, the ECM is composed of significant chemical biology due to variations in protein structure forming the encoded architecture that is the basis for tissue structure and function. Notably, the ECM is a proteinaceous composition with significant post-translational modifications (PTMs). The ECM functions as a dynamic molecular highway for cellular signaling *via* control of chemical gradients, mechanotransduction, protein–protein interactions, receptor binding, and protease-induced remodeling [1–6]. Proteins that comprise the ECM include collagens, elastin, glycoproteins, proteoglycan proteins, and enzymes such as matrix metalloproteinases (MMPs) and lysyl oxidases that assemble structure outside of the cell [7,8]. The structure and composition of the extracellular microenvironment are controlled by deposition of collagen superstructures and secretion of other

Abbreviations
AFM, atomic force microscopy; ColXaY, alpha Y chain of collagen type X; DDA, data-dependent acquisition; DESI, desorption electrospray ionization; DIA, data-independent acquisition; ECM, extracellular matrix; FFPE, formalin-fixed paraffin-embedded; H&E, hematoxylin and eosin; HYP, hydroxylation of proline or hydroxylated proline; IHC, immunohistochemistry; IR-MALDESI, infrared-matrix-assisted laser/desorption electrospray ionization; iTRAQ, isobaric tag for relative and absolute quantitation; LAESI, laser ablation electrospray ionization; LC–MS/MS, liquid chromatography tandem mass spectrometry; LOX, lysine oxidase; LOXL, lysine oxidase-like; MALDI, matrix-assisted laser/desorption ionization; MIBI, multiplexed ion beam imaging; MMP, matrix metalloproteinase; MRM, multiple reaction monitoring; MSI, mass spectrometry imaging; P3H1, prolyl-3-hydroxylase 1; P4HA, prolyl-4-hydroxylase; PC-MT, photocleavable mass tags; PLOD, lysine hydroxylase; PNGase F, peptide-*N*-glycosidase F; PSR, picrosirius red; PTM, post-translational modification; QconCAT, quantitative concatemers; SALDI, surface-assisted laser/desorption ionization; SDS/PAGE, sodium dodecyl sulfate/polyacrylamide gel electrophoresis; SEM, scanning electron microscopy; SHG, second harmonic generation; SIMS, secondary ion mass spectrometry; SRM, selective reaction monitoring; THR, triple helical region; TMA, tissue microarray; TME, tissue microenvironment; TMT, tandem mass tag; TOF, time of flight.

FEBS Letters **598** (2024) 602–620 © 2024 The Authors. *FEBS Letters* published by John Wiley & Sons Ltd on behalf of Federation of European Biochemical Societies.

This is an open access article under the terms of the Creative Commons Attribution-NonCommercial-NoDerivs License, which permits use and distribution in any medium, provided the original work is properly cited, the use is non-commercial and no modifications or adaptations are made.

extracellular proteins that regulate tissue homeostasis. Collagens are present within almost all of the animal kingdom, forming the basis of structure and function for all organs through multiscale processing from single chain fibrils to suprastructure bundles of fibers [9,10] (Fig. 1). The analysis of structural features of fibrillar collagens, the surrounding extracellular matrix proteins, and chemical composition poses an analytical challenge. This review focuses on proteomic analysis of the ECM to include fibrillar collagens that form the structure of the tissue microenvironment. Collagen synthesis and its role in producing the extracellular structure is discussed to give context to associated analytical hurdles. Methods to visualize the pathology of the extracellular matrix cover historical use of chemical stains and microscopy techniques, chromatographic proteomic approaches, current spatial transcriptomics, and spatial proteomics targeting ECM. A perspective summarizes the potential of the extracellular matrix in the study of human disease.

Extracellular matrix form leads to function

Within the extracellular matrix, collagens form an intricate structural and cell sensory information network that shapes the basis of tissue health. There are 28 members of the remarkably complex collagen family that forms the suprastructure scaffolding throughout the TME [11]. Recent reviews and original studies provide deep detail into the process of extracellular collagen assembly, covered in brief here [9,12–14]. All collagen proteins are characterized by the presence of a unique triple helical quaternary structure with repeat sequences of G-X-P or G-P-X, where X is frequently a nonpolar aliphatic amino acid [15]. This triple helical region encodes multiple protein and cell interactions domains that produce significant cell sensory information [16,17]. Within the triple helical region (THR), proline is the second most abundant amino acid after glycine and is variably modified by hydroxylation, or the insertion of an oxygen, at the 3- or, most commonly, 4-position of the proline residue [18,19]. Hydroxylation of proline (HYP) plays a significant role in hydrogen bonding of the THR [20]. Throughout the tissue microenvironment, HYP site variability controls and modulates the exposure of the collagen suprastructure cell binding domains, resulting in the structure–function relationships of specific organs [21–24]. The addition of the most common modification, 4-hydroxylation of proline, is an enzymatic process critical to collagen synthesis utilizing any one of three cell-specifically produced prolyl-4-hydroxylases (P4HA1, P4HA2, P4HA3), ascorbic acid, iron, oxygen, and succinate to create the HYP site during collagen synthesis

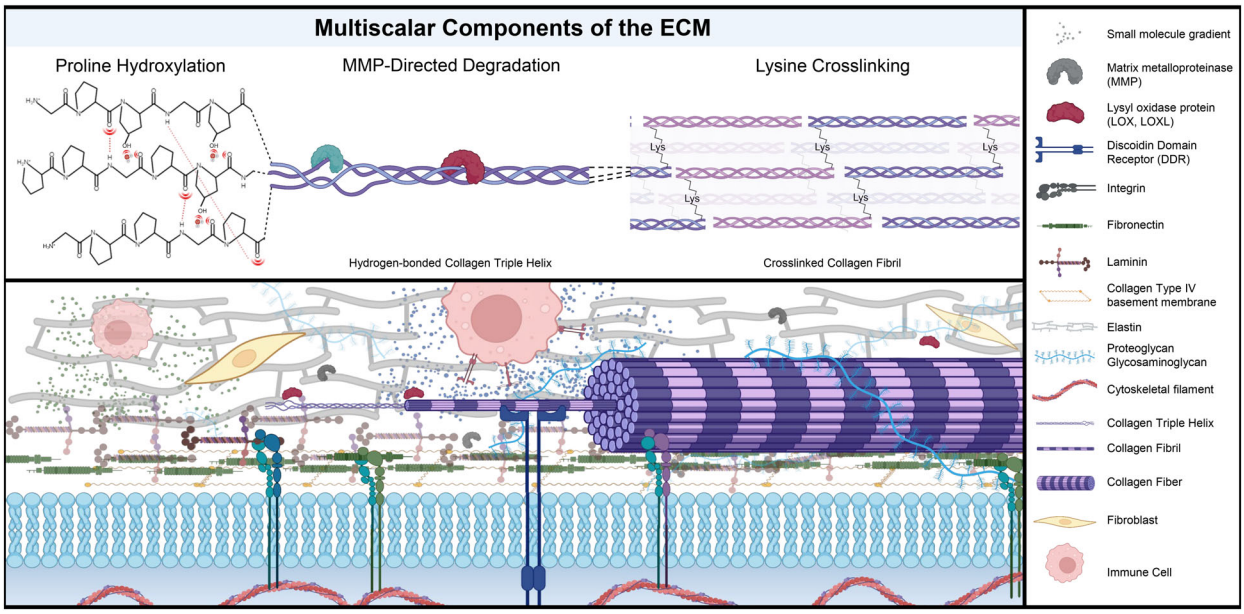

Fig. 1. Multiscalar components of the extracellular matrix and collagen structure. The top schematic depicts processes involved in multiscalar collagen fibril formation and the post-translational modifications that can occur within each structure. Hydrogen bonds are indicated with red semi-circles accompanied by dotted lines pairing hydrogen bond donors and acceptors. The bottom schematic details the multiscalar small molecules, proteins, protein suprastructures, and cells that comprise the extracellular matrix. Together collagen composition and structure form a dynamic extracellular microenvironment.

18733468, 2024, 6, Downloaded from https://febs.onlinelibrary.wiley.com/doi/10.1002/1873-3468.14852, Wiley Online Library on [30/08/2025]. See the Terms and Conditions (https://onlinelibrary.wiley.com/terms-and-conditions) on Wiley Online Library for rules of use; OA articles are governed by the applicable Creative Commons License

[23,25]. Fibrillar collagens have several hundred potential sites for 4-HYP (putative: Col1a1, 283 sites; Col1a2, 237 sites; Col3a1, 286 site; Col5a1, 293 sites), creating potential for an immense amount of variability and structural conformations. The 3-HYP position is more rare in fibrillar collagens, occurring in fewer site residues (6–20 sites mapped [26]) facilitated by prolyl 3-hydroxylase-1 (P3H1) complexing with cartilage-associated protein and cyclophilin B [27]. In early synthesis within the Golgi apparatus, HYP sites are added to single-strand chains [22,28,29]. HYP-facilitated hydrogen bonding occurs after chain combination at the C terminus of single strands to form a triple helical structured propeptide with free strands at the N and C termini [22]. Fibrillar collagen Col1a1 and Col1a2 are frequently combined in a 2 : 1 ratio to form an initial triple helical structure [29,30], yet this ratio is dependent on the biological status of the tissue. After secretion from the cell, fibrillar collagens, now in a triple helical "brick," fuse through enzymatic processes cleaving the N- and C-terminal strands to form insoluble fibrils and fibers with differing width, length, and curvatures. Mechanisms and sequence of assembly driving structural formation within the extracellular microenvironment are somewhat undefined and are due to cell processing and/or mechanical loading [9]. Cellular processing involves, in some ways, the presence of fibropositors or membrane channels that form template spaces for organizing individual or groups of fibrils [31]. Modeling data that included electron microscopy and laser capture microdissection coupled with proteomics suggested that not all assembly is dependent on cellular processes and may be driven by mechanical loading [32]. In this model, free triple helical segments were observed secreted early in development and self-assembled through processes of mechanical loading, and aggregation in the absence of cells [32]. As part of extracellular assembly, crosslinks are formed between collagen types as well as other ECM proteins. Crosslinking occurs through short lived post-translational modifications of lysine hydroxylation, a modification placed by one of three lysyl hydroxylases (PLOD1-3) [33,34]. Disulfide bridge formation by protein disulfide isomerases, glutamate/lysine crosslinks by transglutaminases, and lysine/lysine crosslinking by lysine oxidase (LOX) or lysine oxidase-like proteins (LOXL1-4) form crosslinks within the extracellular space [35–37]. Crosslinking produces ultrasuprastructure scaffolding throughout the TME to present an additional macro level of chemical biology and cell sensory mechanism. The way that fibers assemble within the extracellular microenvironment have been known for decades to alter in disease status [38,39]. Alterations in extracellular assembly are driven by mutations, propeptide splice variants, changes in ECM composition or post-translational modifications, differential crosslinking and MMP activity [30,40–43]. Subsequently, fiber measurements have been used to predict disease progression and outcome [39,44,45]. The variations and scalability of the biology presented throughout collagen synthesis, secretion and modeling direct the cell and structure network of TME form and function. These factors also pose analytical challenges toward understanding the complexity of fibrillar collagen composition and organization within the tissue microenvironment.

Scope of the analytical challenge

The cell processing, composition, and multiscalar combinations of the ECM pose analytical challenges toward evaluating a complete TME that includes the extracellular environment. With the exception of small molecules and minerals, the ECM is primarily composed of proteins with significant contributions from post-translational modifications [46,47]. Post-translational modifications (PTMs) of N-linked glycoproteins and glycosaminoglycans form the basis for gradient control and protein–protein interaction within the ECM PTMs pose analytical challenge through complex structural diversity within glycoform groups, high molecular weight, and a diversity of negatively charged functional groups that can present on the polysaccharides [48,49]. Methods that work to isolate and decellularize the tissue may damage ECM components, distort the amount of soluble ECM used to shape the microenvironment, and lose important spatial secretory information within a cellular niche. Transcription that reports the assortment of potential products is frequently done at a different time scale than the long-lived suprastructure proteins and is unable to report site-specific localization of PTMs. Trypsin, the conventional enzyme used for proteomics, has limited activity against collagen due to suprastructure formation and abundant G-P-X and G-X-P regions with lysine crosslinking. The presence of a significant glycine composition in collagens can produce shorter retention times during chromatographic analysis. The high content and variability in 4- and 3-HYP sites requires analytical approaches that can distinguish peptides with the same mass but with variation on which and where prolines are hydroxylated. The high levels of nonpolar aliphatic amino acids result in differences to ionization and fragmentation potential by mass spectrometry proteomics approaches. MMP activity produces significant variation of ECM protein structure [50] and when combined with the use of trypsin may result in larger numbers of semi-tryptic peptides in database searches. Crosslinking between different ECM proteins means that different strategies are needed

18733468, 2024, 6, Downloaded from https://febs.onlinelibrary.wiley.com/doi/10.1002/1873-3468.14852, Wiley Online Library on [30/08/2025]. See the Terms and Conditions (https://onlinelibrary.wiley.com/terms-and-conditions) on Wiley Online Library for rules of use; OA articles are governed by the applicable Creative Commons License

for database searching, as a single detected peptide may be a combination of several proteins. Spatially, ECM significantly controls the topography of the TME and this has been historically addressed with chemical stains that are ambiguous in reporting molecular composition. The majority of studies in spatial proteomics have mimicked chromatographic studies by using trypsin, resulting in the same limitations as tryptic LC–MS/MS approaches. From the collective information on biological processing of ECM, it is clear that analytical approaches directed at ECM must be proteomic in nature but with significant changes to the standard trypsin proteomic workflow. These changes include implementation of nontraditional proteolytic enzymes, alterations in chromatography based on compositional analysis, capabilities to evaluate complex PTMs and site variation, increased spatial resolution to define cellular neighborhoods, new tools to investigate the signaling response to cell type expression, and unique data base searching approaches.

ECM proteomics by chromatography and mass spectrometry sequencing

The study of ECM proteomics by liquid chromatography coupled to tandem mass spectrometry (LC–MS/MS) has been elegantly summarized to cover the last 10 years [51]. Current techniques in ECM proteomics involve sample preparation techniques to enrich ECM proteins, alternative methods to solubilize and digest ECM for analysis, and specialized ECM methods for mass spectrometry data acquisition, and database tools to identify ECM proteins [52–54].

ECM sample preparation techniques

Extracellular matrix proteomic preparation techniques include ECM enrichment by decellularization or ECM fractionation by solubility and can be followed by SDS/PAGE [51–53,55]. Decellularizing the tissue, or removing the cells, is a first pass enrichment step. For LC–MS/MS proteomics, decellularization is done at the tissue level and must be customized per organ tissue type and disease state [56–58]. This is done by incubating tissue samples in lysis buffers [59] or solutions containing detergents, like sodium dodecyl sulfate (SDS) [55,58,60–63]. The soluble fractions contain cellular proteins, whereas the insoluble fraction is enriched for ECM proteins, including collagen types. The ECM fraction is solubilized with high concentrations of chaotropic agents, like urea or guanidine, and addition of reducing reagents such as dithiothreitol [61,62]. A quantitative detergent-based method has been developed that does not include a decellularization step, and instead fractionates ECM based on solubility into buffers with increasing salt and detergent (SDS) concentration [64].

ECM digestion techniques

After ECM enrichment, ECM proteins are digested prior to LC–MS/MS analysis. Typical proteomics techniques rely on trypsin, an enzyme that cleaves at lysine and arginine residues that are not flanked by prolines, to digest a diverse range of proteins. The high proline content of collagens, dense post-translational modifications, and crosslinked insoluble fibers make relatively resistant to trypsin and can result in limited coverage of collagen-type proteins. Glycosylation is a significant PTM within the ECM and poses significant steric hindrance. To improve steric access to the protein structure, ECM-targeted methods have implemented deglycosylation with Peptide N Glycosidase F (removing N-linked glycans) [62,65,66], chondroitinase ABC [67], keratanase, or heparanase [60] (removing glycosaminoglycans) prior to digestion. For increased targeting and access to differential protein structure, alternate enzymes and non-enzyme approaches have been used alone or in combination with trypsin. These approaches include collagenase [58,68,69], pepsin [67], or LysC [61,64,65] and chemical digestion by hydroxylamine and cyanogen bromide [70,71].

ECM LC–MS/MS data acquisition and analysis techniques

LC–MS/MS experiments for ECM currently leverage similar proteomics approaches as used in other cellular fractionation methods. Chromatographic approaches use combinations of reverse phase, strong cation exchange and may be used in combination with SDS/PAGE. Acquisition strategies that include data-dependent acquisition (DDA) to produce proteomic libraries are useful in targeted regional analysis [72] and with non-tryptic enzymes [68,73]. Data-independent acquisition (DIA) is useful on tryptic digests of ECM, increasing reproducible peptide identification and increasing coverage of the tryptic matrisome [74]. Quantification methods using tandem mass tags (TMT) [75], isobaric peptide labeling (iTRAQ) [76], selective reaction monitoring (SRM) [70], multiple reaction monitoring (MRM) [77], and quantitative concatemers (QconCATs) [78–80] have been employed to understand ECM protein regulation. Significantly, matrisome databases and data tools have been created to collect curated studies of the ECM

18733468, 2024, 6, Downloaded from https://febs.onlinelibrary.wiley.com/doi/10.1002/1873-3468.14852, Wiley Online Library on [30/08/2025]. See the Terms and Conditions (https://onlinelibrary.wiley.com/terms-and-conditions) on Wiley Online Library for rules of use; OA articles are governed by the applicable Creative Commons License

across tissue types, with visualization of PTM and structural entities [54,81,82].

Spatial analysis of the extracellular microenvironment

Spatial analysis works to report relationships between single cell types to cellular neighborhoods throughout the TME. The extracellular microenvironment represents an important component of this crosstalk. The emergence of spatial biology has now resulted in a plethora of techniques focused on detecting single cells, yet less so on defining the *in situ* molecular components of the extracellular microenvironment that provide functional communication between cells. Historically, chemical staining has been the most common way to gain spatial information on the extracellular microenvironment. Chemical stains (Table 1) combined with microscopy methods target collagen structure and report distribution, intensity, and fiber measurements. Electron and photon microscopy techniques use the birefringent properties of the extracellular matrix to produce high spatial resolution images of collagen fibers surrounding tissue features or within cellular regions. Spatial transcriptomics and proteomics work to detect multiplexed combinations of extracellular components at the transcript level or protein level. New techniques in spatial proteomics leverage mass spectrometry imaging to target and access the ECM proteome (Fig. 2). Current trends in spatial omics are emerging to combine all of these techniques as multimodal, multiplexed studies to form a complete systems biology portrait of the TME. This section discusses historical and current trends in the spatial analysis of the extracellular microenvironment.

Chemical stains

The Hematoxylin and Eosin (H&E) stain is considered the gold standard for clinical applications and has been used in pathological workflows to diagnose diseases. H&E was one of the first stains reported for use on connective tissue in 1876 [83]. Hematoxylin or its oxidized form, hematein, is a stain initially extracted and synthesized from the logwood tree [84,85]. It binds to negatively charged DNA and RNA molecules, staining nuclei purple. The hematoxylin stain comes in many forms based on the oxidizer and mordant used. The water-soluble and acid-resistant properties of hematoxylin make it compatible with downstream acidic counterstains [86]. The most common hematoxylin used in H&E stains is Mayer's hematoxylin, which is oxidized by sodium iodate and uses potassium or ammonium aluminum sulfate. Eosin is ethanol-soluble and stains collagenous, muscle fibers, and cytoplasm pink [87]. Combined H&E can stain with up to five shades of pink, providing information on cellular morphology as well as distribution and patterning of collagen features [86,88]. H&E cannot distinguish types of collagen. H&E may be used with Second Harmonic Generation microscopy to report collagen fiber measurements (length, width, curvature) related to features within the TME [89].

Masson's Trichrome staining was first published in 1929 [90] and involves a nuclear stain (Weigert's hematoxylin: brown/black), a cytoplasmic and muscular tissue stain (acid fuchsin with ponceau: red) and a connective tissue stain (aniline blue (methyl blue): blue or green) [91]. It is shown to stain collagens blue or green dependent on basic residues as well as muscle fibers red or yellow depending on their maturity [92]. Masson's Trichrome staining has been used to stain collagen and assess its structure and organization [93,94] and is oftentimes used alongside other ECM imaging techniques such as immunohistochemistry, second harmonic generation, and other imaging modalities [95–98].

Saffron, which comes from the stigmata of the saffron flower, stains collagen fibers yellow and is typically used in conjunction with hematoxylin and either eosin [99,100] or, in earlier years, phloxine [101,102]. Saffron is also one of the five stains in Movat's pentachrome stain., This stain dyes acidic carbohydrates blue (Alcian Blue), nuclei black (Weigert's hematoxylin), elastin dark purple (resorcin-fuschin), muscle and fibrinoid red (woodstain-scarlet-acid fuchsin), and collagen fibers yellow (saffron) [103]. Saffron stains may be used as a single stain or in combination to quantify collagen fibers by a yellow intensity readout [104].

Herovici's picropolychrome stain [105] stains muscle fibers and cytoplasm yellow (picric acid), and produces either a fuchsia/red (acid fuchsin) or blue (methyl blue) staining in collagenous regions [106,107]. Methyl blue is pH-dependent, binding to exposed basic sites, leading to the characteristic that blue stains represent immature collagen fibers. The exact target composition of the Herovici stain remains undefined. Herovici's stain has been used to report and relatively quantify Collagen Types I and III as well as immature and mature collagen [108–113], with controversy regarding the type of collagen that is stained.

Picrosirius Red (PSR) [114] selectively stains collagens reddish orange. The binding mechanisms have been shown to be electrostatic, meaning the dye can be removed with a low pH [115]. Combining PSR with the use of a polarized filter in microscopy can enhance

18733468, 2024, 6, Downloaded from https://febs.onlinelibrary.wiley.com/doi/10.1002/1873-3468.14852, Wiley Online Library on [30/08/2025]. See the Terms and Conditions (https://onlinelibrary.wiley.com/terms-and-conditions) on Wiley Online Library for rules of use; OA articles are governed by the applicable Creative Commons License

Table 1. Chemical stains for extracellular matrix visualization. Staining reagents that comprise the dye, their staining substrates, and the resulting color of the stained substrates are summarized. If known, staining reagent properties, such as acidity or basicity, optimal staining pH, and proposed staining mechanism are listed.

	Staining reagents	Substrates stained	Color	Staining mechanism (optimal pH)	First used
Hematoxylin & Eosin	Mayer's Hematoxylin (Potassium or ammonium aluminum sulfate mordant, sodium iodate oxidation)	Nuclei, rough ER, ribosomes	Black	Basic dye (pH 2.4–2.9) Binds negatively charged residues (DNA) [85]	1876
	Eosin	Cytoplasm, ECM	Pink	Acidic dye (pH 5.0) Binds basic residues	
Masson's trichrome	Weigert's Hematoxylin (Ferric chloride mordant, natural oxidation)	Nuclei, rough ER, ribosomes	Black	Basic dye (pH 2.4–2.9) Binds negatively charged residues (DNA) [85]	1929
	Acid Fuchsin with Ponceau	Cytoplasm and connective tissue	Red	Acidic dye (2.5) Binds basic residues [115]	
	Aniline blue (methyl blue and Water blue)	Collagens	Blue	Acidic dye	
Movat's pentachrome	Weigert's or Verhoeff's Hematoxylin (ferric chloride mordant, natural or iodine oxidation)	Nuclei	Black	Basic dye (pH 2.4–2.9) Binds negatively charged residues (DNA) [85]	1955
	Saffron	Collagen	Yellow	Unknown	
	Alcian Blue (Methylene blue)	Polysaccharides	Blue	Basic dye (pH 2.5) Binds protonated acidic residues (–HSO4 and –OH)	
	Acid Fuchsin	Muscle Fibers	Red	Acidic dye Binds basic residues [115]	
	Crocein	Fibrin	Bright Red	Unknown	
Herovici	Weigert's Hematoxylin (Ferric Chloride Mordant, natural oxidation)	Nuclei, Rough ER, Ribosomes	Black	Basic dye (pH 2.4–2.9) Binds negatively charged residues (DNA) [85]	1963
	Acid Fuchsin with picric acid	Muscle Fibers	Red	Acidic dye Binds basic residues [115]	
	Aniline blue (methyl blue and Water blue)	Collagens	Blue	Acidic dye	
Picrosirius Red	Weigert's Hematoxylin (ferric chloride mordant, natural oxidation)	Nuclei, rough ER, ribosomes	Black	Basic dye (pH 2.4–2.9) Binds negatively charged residues (DNA) [85]	1968
	Sirius red (Red 80) with picric acid	Collagens	Birefringent Yellow-red	Acidic dye Binds basic residues [115] Binds parallel to collagen fibers [207]	

birefringence of finer collagen fibers and aid in reporting collagen organization across the tissue. The ability of PSR to distinguish between collagen types remains undefined [116,117].

Atomic/electron/photon microscopy techniques for fiber measurement

Microscopy techniques for assessing collagen fibers and overall ECM organization include atomic force microscopy (AFM), scanning electron microscopy (SEM) and second harmonic generation (SHG) [38,118,119]. These techniques do not chemically alter or ablate tissues, making them compatible with downstream analyses. In AFM, a mechanical probe is scanned across the surface of tissues and cantilever movements are detected to provide a three-dimensional image of a tissue's surface with a lateral resolution of 1 nm and a vertical resolution of 0.1 nm [120]. AFM may be used to spatially assess physical properties including stiffness, elasticity, and adhesion [121]. In SEM, a high-energy beam of

18733468, 2024, 6, Downloaded from https://febs.onlinelibrary.wiley.com/doi/10.1002/1873-3468.14852, Wiley Online Library on [30/08/2025]. See the Terms and Conditions (https://onlinelibrary.wiley.com/terms-and-conditions) on Wiley Online Library for rules of use; OA articles are governed by the applicable Creative Commons License

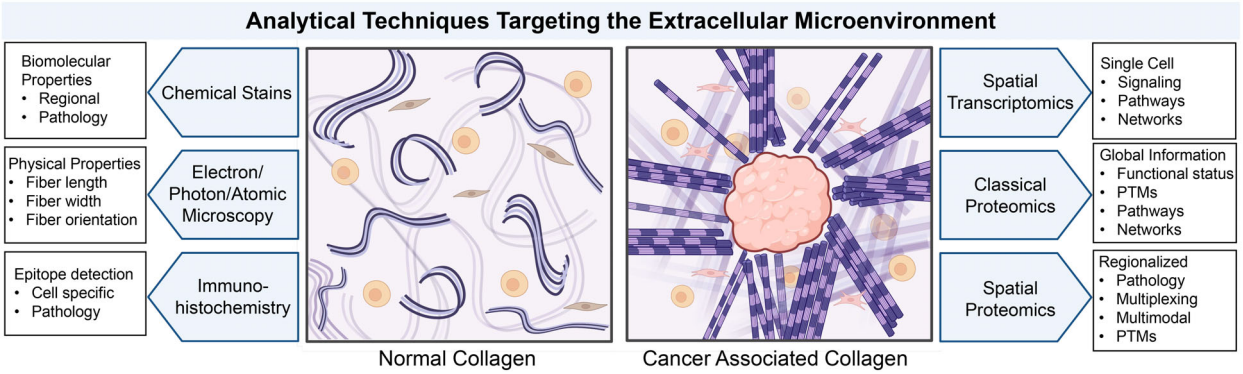

Fig. 2. Approaches to analyzing multiscalar features of the extracellular microenvironment including collagen fibers. An assortment of analytical techniques has been used to probe the molecular and physical composition of the ECM. PTMs, post-translational modifications.

electrons is stepped across unstained, thinly cut tissue sections [122,123]. The readout is emitted, diffracted, and backscattered electrons focused through lenses and detected by a secondary electron detector. SEM resolution depends on the incident probe diameter and can produce features as small as 1 nm. In SHG, irradiation of tissue results in two incident photons with the same frequency simultaneously impacting a birefringent material, creating the emission of one photon with twice the frequency and same direction propagation as the incident photons [124,125]. When imaged with a lens that filters for the second harmonic wavelength, the resulting image allows quantitative analysis of the distribution, shape, and orientation of collagens [126]. SHG microscopy resolution depends on the excitation wavelength, which typically ranges from 400 to 1000 nm [127]. There are numerous variations of SHG microscopy that work to measure the different physical properties arising from irradiation of birefringent extracellular matrix [125]. SHG has also been multiplexed with two-photon microscopy (multiphoton imaging) to visualize collagens within surrounding tissue architecture and with H&E staining to co-register collagen fiber information with pathological features [128–130].

Spatial transcriptomics

Spatial transcriptomics allows for spatially distributed expression profiles of RNA within fixed or frozen tissue sections with a diversity of workflows [131–137]. A general workflow uses UV labile oligonucleotides tags on antibodies or *in situ* hybridization probes to bind to target RNA or proteins over the entire tissue section. In certain workflows, regions of interest may be identified by fluorescently labeled antibody markers of the cell types of interest. The areas of interest are irradiated with UV light, which releases probes for amplification (GeoMx Digital Spatial Profiler, Nanostring). This process can produce spatial information from single cells to thousands of cells with multiplexed information at the protein and genetic level. In most cases, the tissue must be placed onto a specified target area, which requires access to stored tissue blocks for specialized sectioning. Commercialization of these techniques has increased the accessibility for multiplexed studies that include ECM profiles. Spatial transcriptomics lacks information on protein composition and post-translational modification. Timing between transcription and modeling of the ECM may be vastly different [138,139].

Multiplexed imaging by antibodies

Multiplexed antibody approaches target specific protein through antibody binding epitopes down to single cell levels. These approaches use fast mass spectrometry analyzers, such as time of flight (TOF), paired with detectors, such as multichannel detectors [140,141], that are capable of capturing multiplexed signal. Mass cytometry [142,143] or CyTOF® uses antibodies coupled with rare metal tags irradiated by a laser beam to visualize single cells down to 1 μm within the TME. Mass cytometry is generally restricted to a small area around 800 μm^2 where the tissue is completely ablated during analysis. Multiplexed Ion Beam Imaging (MIBI-TOF) [144,145] uses combinations of rare metals detected by stepping an ion beam composed of oxygen ions (O_2^+) [146] across the surface to release the tags. MIBI-TOF works within a select region around 800 μm^2 and has a spatial resolution of < 200 nm. MIBI-TOF is a surface scan, removing the top molecular layers for analysis. Photocleavable mass tags (PC-MTs) are a recent development that can be leveraged

18733468, 2024, 6, Downloaded from https://febs.onlinelibrary.wiley.com/doi/10.1002/1873-3468.14852, Wiley Online Library on [30/08/2025]. See the Terms and Conditions (https://onlinelibrary.wiley.com/terms-and-conditions) on Wiley Online Library for rules of use; OA articles are governed by the applicable Creative Commons License

for multiplexed studies by any mass spectrometry instrument equipped with a matrix-assisted laser desorption/ionization (MALDI) source [147]. PC-MTs on antibodies are applied to the entire tissue, released by brief exposure to UV light and the tags detected in place after application of a chemical matrix that facilitates ionization. PC-MT may be used to evaluate entire tissue sections to smaller, high spatial resolution regions [148] and are likely compatible with other sources such as desorption electrospray ionization. A pitfall with all antibody approaches is that the mechanism of detection involves binding to a specific epitope within the protein structure. This greatly limits detection of detailed protein domain modulation, including post-translational modifications.

Laser capture microdissection coupled to proteomics

In this approach, a laser is used to isolate a small region, which is then captured and processed by microproteomics techniques [149]. Microproteomics typically uses the same enzymatic approaches and chromatography techniques in as in conventional proteomics studies. Current studies leverage using multiplexed markers of disease to target specific regions for microproteomics [72,150]. This is a powerful approach for comprehensive proteomic assessment of the ECM, especially when paired with other modalities such as SEM or nonlinear birefringent techniques [32]. An advantage is the proteomic depth achieved by microproteomics when compared to other tissue imaging proteomics. A main limitation is that removal of the region limits understanding the association with the surrounding tissue and the removed regions cannot be used for further multiplexed targeting of specific analytes.

Mass spectrometry imaging of ECM

Mass spectrometry imaging (MSI) has been used for decades to investigate the spatial distribution of many types of analytes [151–153]. Mass spectrometry imaging requires a source capable of focusing on a discrete x and y coordinate for downstream analysis and detection. The source is stepped across the tissue or two-dimensional target in an array fashion and at each x and y coordinate produces a mass spectrum that contains hundreds to thousands of analyte peaks. Each peak represents an image channel that can be mapped across the entire tissue section. There are many sample preparation approaches dependent on the study hypothesis and configurations of mass spectrometry instrumentation [154–156]. This review reports on detection of ECM by MSI, which we term ECM-MSI.

Ionization sources

Many different ionization methods that have been developed in the field of mass spectrometry imaging (MSI). Secondary ion mass spectrometry (SIMS) has been used to spatially profile ECM proteins [157]. Other ionization techniques initially used for small molecule analysis that have recently been optimized to image peptides and proteins, but have yet to explore the ECM include infrared-matrix-assisted laser desorption electrospray ionization (IR-MALDESI, small peptides [158,159] and glycans [160]), surface-assisted laser desorption ionization (SALDI [161,162]), desorption electrospray ionization (DESI [163–165] and nano-DESI [166–169]), and laser ablation electrospray ionization (LAESI) [170,171]. MALDI-MSI has been used as a main approach to peptides derived from the ECM by mass spectrometry imaging [68,172]. This review will focus on the use of matrix-assisted laser desorption/ionization mass spectrometry imaging (MALDI-MSI) for ECM analysis.

Considerations for ECM sample preparation and peptide identification by ECM-MSI

Accessing the extracellular matrix proteome by MALDI-MSI leverages enzyme specificity to produce analytes from target protein structure. MALDI-MSI may be done as a single analytical approach or used with multimodal, multiplexed strategies to visualize the ECM (Fig. 3). The image data obtained by MALDI-MSI of the ECM contains spatial distribution of peptides produced from enzymatic digestion of targeted protein structures. Identification is done after MALDI-MSI in a separate step on the same tissue section [68,173]. The workflow is highly synchronous with immunohistochemistry approaches [68,155,173]. Enzymes may be used on fresh-frozen tissue or fixed tissue and are sprayed onto the tissue using automated sprayers to maintain localization. Fresh-frozen tissue requires clearing of metabolites and lipids prior to enzymatic digestion, whereas formalin-fixed tissue requires additional steps that remove the formalin crosslinks between proteins by antigen retrieval [172,174,175]. Both clearing and antigen retrieval are required to increase access to the protein structure. The general workflow includes tissue clearing and/or antigen retrieval, enzymatic spraying and digestion, chemical matrix application for ionization (oftentimes α-cyano-4-hydroxycinnamic acid for proteins and peptides), and mass spectrometry data acquisition. Improvements in instrumentation and sample preparation have allowed for increases in sensitivity,

18733468, 2024, 6, Downloaded from https://febs.onlinelibrary.wiley.com/doi/10.1002/1873-3468.14852, Wiley Online Library on [30/08/2025]. See the Terms and Conditions (https://onlinelibrary.wiley.com/terms-and-conditions) on Wiley Online Library for rules of use; OA articles are governed by the applicable Creative Commons License

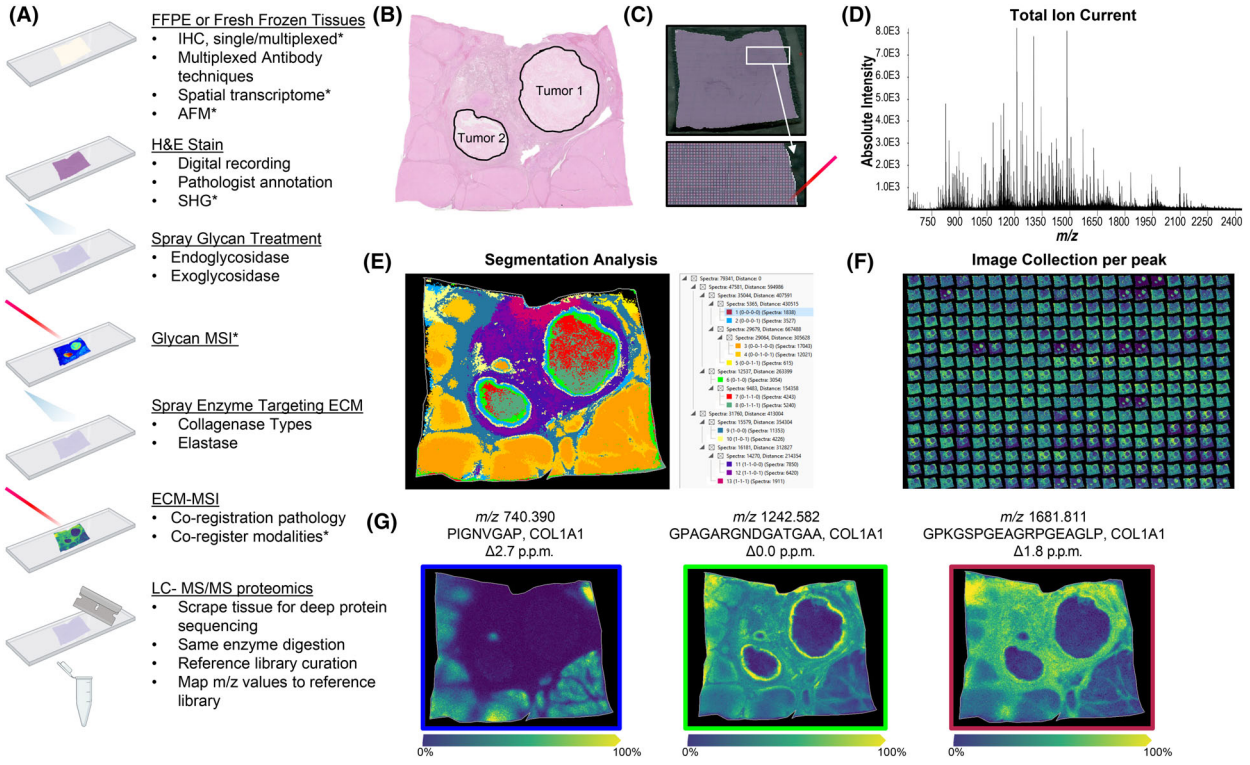

Fig. 3. Integrative MALDI-MSI targeting the extracellular microenvironment. (A) Overall Spatial Imaging Workflow by MALDI-MSI. MALDI mass spectrometry imaging workflow details integral steps in matrix proteome imaging tissues on standard microscope slides by charge decoupled sources. Steps that are depicted are indicated with a black outline. * designates optional techniques that can be performed throughout the workflow on the same tissue section are included at optimal locations within the workflow. Techniques discussed performed prior to MALDI-MSI of ECM include GeoMx, MALDI-immunohistochemistry (IHC), second harmonic generation microscopy (SHG), scanning electron microscopy (SEM), immunohistochemistry (IHC) and atomic force microscopy (AFM). (B) Hematoxylin and eosin (H&E) stains are pathologically annotated. H&E-staining of a representative formalin-fixed paraffin-embedded (FFPE) hepatocellular carcinoma tissue section enables pathological annotation of tumor (black) and stroma (blue) regions. (C) Tissues are sampled at discrete points with a laser. Shown are the designated sites where the laser will sample the tissue prior to actual acquisition. (D) Mass spectra are produced from each pixel. A MALDI mass spectrum shows representative mass range and *m/z* values detected from ECM-MSI. (E) Heuristic spatial clustering produces localized ECM proteomes. Example segmentation image analysis was produced from mass spectra from 79 341 pixels. Segments were produced from heuristic spatial clustering using bisecting *k*-means and the Manhattan metric. A legend of the cluster analysis is shown on the right. (F) Multiplexed image collection. Example of 280 MALDI-MS images representing a fraction of the peptides detected in tissue with high levels of stroma. (G) Mass spectrometry images are produced from individual *m/z* values. Images are matched by high mass accuracy to peptides derived from LC–MS/MS of the same tissue section. Individual MALDI-MS images show spatial distribution of peptides with *m/z* values of 740.390 (P740), 1242.582 (P1242), and 1681.811 (P1681). Yellow indicates high peptide intensity and blue indicates low peptide intensity.

throughput, mass accuracy, and resolution. Considerations for customizing sample preparation include the type of tissue being imaged, the enzymes used for targeting the ECM proteins or PTMs and required spatial resolution. MALDI ECM-MSI has been done on fresh-frozen tissues, formalin-fixed paraffin-embedded (FFPE) [68,176–178] tissues, and tissue microarrays (TMAs) [179–183]. Embedded tissues or TMAs are sectioned with a typical thickness of 3–7 µm for FFPE tissues and 8–10 µm for fresh-frozen tissues [173,184]. It should be noted that tissue thickness has been shown to alter MALDI-MSI peak intensities in FFPE tissues [185]. The type of instrument available dictates the type of substrate the sample may be mounted on. For charge decoupled sources where MALDI is coupled with an ion funnel, a standard microscope slide may be used. In our group, very little charge build-up has been observed over hundreds of slides analyzed. For charge coupled sources (MALDI-TOF), a conductive slide must be used, typically an indium tin oxide coated; these slides are commercially available. Decellularization may be done on fresh-frozen samples at the tissue or organ level to enrich ECM proteins prior to enzymatic digestion [186]. Enzymatic

18733468, 2024, 6, Downloaded from https://febs.onlinelibrary.wiley.com/doi/10.1002/1873-3468.14852, Wiley Online Library on [30/08/2025]. See the Terms and Conditions (https://onlinelibrary.wiley.com/terms-and-conditions) on Wiley Online Library for rules of use; OA articles are governed by the applicable Creative Commons License

techniques used to report spatial distribution of the ECM include untargeted approaches using trypsin [172] or pepsin [187], and targeted approaches using elastase (elastin) [68,188], PNGase F (N-linked glycans) [189], EndoF (core-fucosylated N-glycans) [190], chondroitinase ABC (chondroitins) [191], isoamylase (glycogen) [192], or collagenase (collagens and 40–60 other ECM proteins) [68]. When choosing enzymes, it is important to consider the consensus site of the target. Tryptic digests of proline-rich proteins, like collagen, show reduced coverage when compared to proteins with lower proline content due to limited cleavage when lysine/arginine is followed by a proline residue [193]. N-linked glycosylation is restricted by consensus site to N-X-S/T, where X cannot be proline. Fibrillary collagens have limited consensus sites; however, more than 75% of ECM proteins surrounding the collagens are N-linked glycosylated and have on average 4.3 N-linked consensus sites. Deglycosylation greatly improves access to the ECM protein structure for increased detection of ECM proteins [194]. Spatial studies reporting ECM expression have used either trypsin [176–178,182,195] or collagenase Type III [68,180,181,191,194,196–198] in combination with deglycosylation.

A challenge with ECM-MSI is that identification is done in a separate workflow but on the same tissue section, creating a reference library to match by accurate mass or using targeted approach to sequence a peptide or analyte of interest. Targeted identification can be done by on-tissue MALDI-MS/MS [179,199], or by using an in silico reference library [182,183]. Using the same tissue section, an untargeted reference library may be created by LC–MS/MS from either locally-digested, liquid-extracted peptides [177] or in-solution-digested peptides from homogenized whole tissue [178,196] or homogenized macrodissected regions of interest [176].

Multimodal multiplexing with ECM spatial proteomics by MALDI-MSI

An advantage ECM-MSI is that any of the enzymes may be used in serial with careful planning and with other omic approaches, thus producing a more complete view of the TME. This has been done with combinations of glycans, chondroitins, tryptic peptides, elastase peptides, and collagenase peptides [191,200–202]. Single and multiplexed enzymes are highly compatible with common pathology stains, including H&E, done on the same tissue section [194,203]. This opens the prospect for multimodal approaches that combine photon microscopy such as second harmonic generation toward investigating collagen fiber measurements. Immunohistochemistry is a well-established approach that probes epitopes of interest with primary antibodies. Their presence is detected by a chromophoric readout produced either directly from the primary antibody or indirectly through a conjugated secondary antibody. Immunohistochemistry (IHC) and MALDI-MSI has been used together to further validate findings and increase biological information associated with the study [176,182,183,195,204,205]. ECM-MSI using collagenase and IHC can be performed on the same FFPE tissue section with high reproducibility and without reduction in downstream ECM signal compared to unstained tissue sections [196]. A comprehensive multimodal multiplexing study on same tissue sections was recently completed evaluating single cell type approaches GeoMx Digital Spatial Profiling, CyTOF, and PC-MTs (Ambergen) in combination with multiplexed ECM-MSI by PNGase F to release N-glycans and collagenase to target the ECM [206]. Single cell type approaches were used as "drop-in" methods without modifying the manufacturer's protocols to evaluate placement in the workflow. The overall conclusion was that antibody-directed workflows were done best as a first step prior to ECM-MSI. Combining modalities produces a complete view of cellular and extracellular imaging data and provides context on how specific cell types function within the surrounding extracellular microenvironment.

Perspective

The analysis of both the cellular and extracellular microenvironment presents a holistic view of the TME with enormous potential to impact human health (Fig. 4). The matrisome remains a complexity of post-translational modifications, mutations, splice variants, translational variation and regulation, crosslinking, and remodeling that we have simply not defined in depth at any one point. All of these variables of the matrisome can differ for each organ. A significant part of the problem is that the tools needed for a complete investigation of the tissue microenvironment that include the extracellular microenvironment have not been developed. Enzymes, not antibodies, represent considerable tools for targeting the extracellular matrix proteome. Multiplexed enzymatic approaches may be used either collectively or in serial to systematically define the matrisome. Although we have at hand spatial approaches to define the extracellular matrix "unit" along with cell signaling and composition, work needs to be done to fully integrate these modalities from analytics to data reporting and visualization.

18733468, 2024, 6, Downloaded from https://febs.onlinelibrary.wiley.com/doi/10.1002/1873-3468.14852, Wiley Online Library on [30/08/2025]. See the Terms and Conditions (https://onlinelibrary.wiley.com/terms-and-conditions) on Wiley Online Library for rules of use; OA articles are governed by the applicable Creative Commons License

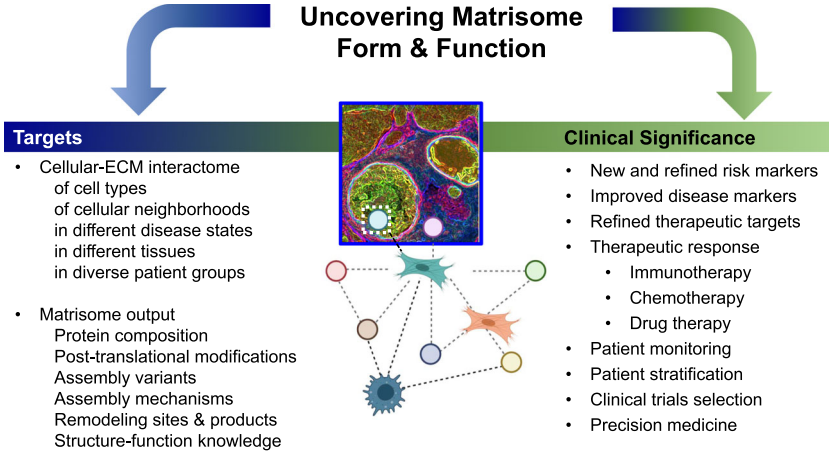

Fig. 4. Perspective on where continued work is needed on cell-ECM interactions, matrisome output and the clinical utility of the matrisome.

These integrative cell and ECM units would be best represented at a systems biology level, where across the tissue topography, one can report the cell interactive neighborhood along with ECM form and function. Collagen proteins should be represented as networked structures rather than single entities as it is the domain regulation that reflects tissue function. At a cellular level, we understand very little about how each cell type produces the cell-specific extracellular microenvironment. The interactive neighborhood specifically of fibroblast subtypes remains undefined and immense knowledge remains to be gained from how the fibroblast interactome responds to other cell types, especially immune cells, in different tissue and disease states. All current proteomic studies are limited in differentiating the secretory or waste products of the cells extruded into the extracellular space or proximal fluid, and this presents a novel reservoir for disease markers. Many diseases are driven by changes in ECM deposition, yet the clinical significance of the matrisome remains largely untapped. It is expected that mining of the matrisome, especially with spatial data, will produce novel risk to progression markers, refine therapeutic targets, report on therapeutic response, and stratify for clinical trials selection. With this in mind, the spatial matrisome presents a critical part of precision medicine but is, as of yet, a nearly unexplored frontier.

Acknowledgements

JKM was supported by the Cellular, Biochemical and Molecular Sciences Training Program 5T32GM132055 (NIH/NIGMS). PMA was supported by NIH/NCI R01CA253460; P20GM103542 (NIH/NIGMS) and in part by Hollings Cancer Center Support Grant P30 CA138313 at the Medical University of South Carolina. Supported in part by the Biorepository & Tissue Analysis Shared Resource, Hollings Cancer Center, Medical University of South Carolina (P30 CA138313) and MUSC Digestive Disease Research Center (P30 DK123704) (NIH/NIDDK). We appreciate assistance from Jaclyn Dunne scanning H&Es for figures. The contents are solely the responsibility of the authors and do not necessarily represent the official views of the NIH or NCATS. Figures were created with the help of BioRender.com.

References

1 Leitinger B (2003) Molecular analysis of collagen binding by the human discoidin domain receptors, DDR1 and DDR2 identification of collagen binding sites in DDR2. *J Biol Chem* **278**, 16761–16769.
2 Humphrey JD, Dufresne ER and Schwartz MA (2014) Mechanotransduction and extracellular matrix homeostasis. *Nat Rev Mol Cell Biol* **15**, 802–812.
3 Hamaia S and Farndale RW (2014) Integrin recognition motifs in the human collagens. *Adv Exp Med Biol* **819**, 127–142.
4 Su H, Yang F, Fu R, Trinh B, Sun N, Liu J, Kumar A, Baglieri J, Siruno J, Le M *et al.* (2022) Collagenolysis-dependent DDR1 signalling dictates pancreatic cancer outcome. *Nature* **610**, 366–372.
5 Hastings JF, Skhinas JN, Fey D, Croucher DR and Cox TR (2019) The extracellular matrix as a key regulator of intracellular signalling networks. *Br J Pharmacol* **176**, 82–92.
6 Theocharis AD, Manou D and Karamanos NK (2019) The extracellular matrix as a multitasking player in disease. *FEBS J* **286**, 2830–2869.
7 Kular JK, Basu S and Sharma RI (2014) The extracellular matrix: structure, composition, age-related differences, tools for analysis and applications for tissue engineering. *J Tissue Eng* **5**, 2041731414557112.
8 Karamanos NK, Theocharis AD, Piperigkou Z, Manou D, Passi A, Skandalis SS, Vynios DH, Orian-

18733468, 2024, 6, Downloaded from https://febs.onlinelibrary.wiley.com/doi/10.1002/1873-3468.14852, Wiley Online Library on [30/08/2025]. See the Terms and Conditions (https://onlinelibrary.wiley.com/terms-and-conditions) on Wiley Online Library for rules of use; OA articles are governed by the applicable Creative Commons License

Rousseau V, Ricard-Blum S and Schmelzer CEH (2021) A guide to the composition and functions of the extracellular matrix. *FEBS J* **288**, 6850–6912.
9 Revell CK, Jensen OE, Shearer T, Lu Y, Holmes DF and Kadler KE (2021) Collagen fibril assembly: new approaches to unanswered questions. *Matrix Biol Plus* **12**, 100079.
10 Exposito J-Y, Valcourt U, Cluzel C and Lethias C (2010) The fibrillar collagen family. *Int J Mol Sci* **11**, 407–426.
11 Ricard-Blum S (2011) The collagen family. *Cold Spring Harb Perspect Biol* **3**, a004978.
12 Sun B (2021) The mechanics of fibrillar collagen extracellular matrix. *Cell Rep Phys Sci* **2**, 100515.
13 Mouw JK, Ou G and Weaver VM (2014) Extracellular matrix assembly: a multiscale deconstruction. *Nat Rev Mol Cell Biol* **15**, 771–785.
14 Leo L, Bridelli MG and Polverini E (2019) Insight on collagen self-assembly mechanisms by coupling molecular dynamics and UV spectroscopy techniques. *Biophys Chem* **253**, 106224.
15 Gustavson KH (1955) The function of hydroxyproline in collagens. *Nature* **175**, 70–74.
16 Sweeney SM, Orgel JP, Fertala A, McAuliffe JD, Turner KR, Di Lullo GA, Chen S, Antipova O, Perumal S and Ala-Kokko L (2008) Candidate cell and matrix interaction domains on the collagen fibril, the predominant protein of vertebrates. *J Biol Chem* **283**, 21187–21197.
17 San Antonio JD, Jacenko O, Fertala A and Orgel JPRO (2020) Collagen structure-function mapping informs applications for regenerative medicine. *Bioengineering* **8**, 3.
18 Greenberg J, Fishman L and Levy M (1964) Positions of amino acids in mixed peptides produced from collagen by the action of collagenase. *Biochemistry* **3**, 1826–1831.
19 Ogle JD, Arlinghaus RB and Logan MA (1962) 3-Hydroxyproline, a new amino acid of collagen. *J Biol Chem* **237**, 3667–3673.
20 Barth D, Milbradt AG, Renner C and Moroder L (2004) A (4R)-or a (4S)-fluoroproline residue in position Xaa of the (Xaa-Yaa-Gly) collagen repeat severely affects triple-helix formation. *Chembiochem* **5**, 79–86.
21 Krane SM (2008) The importance of proline residues in the structure, stability and susceptibility to proteolytic degradation of collagens. *Amino Acids* **35**, 703–710.
22 Shoulders MD and Raines RT (2009) Collagen structure and stability. *Annu Rev Biochem* **78**, 929–958.
23 Rappu P, Salo AM, Myllyharju J and Heino J (2019) Role of prolyl hydroxylation in the molecular interactions of collagens. *Essays Biochem* **63**, 325–335.
24 Sipilä KH, Drushinin K, Rappu P, Jokinen J, Salminen TA, Salo AM, Käpylä J, Myllyharju J and Heino J (2018) Proline hydroxylation in collagen supports integrin binding by two distinct mechanisms. *J Biol Chem* **293**, 7645–7658.
25 Gorres KL and Raines RT (2010) Prolyl 4-hydroxylase. *Crit Rev Biochem Mol Biol* **45**, 106–124.
26 Weis MA, Hudson DM, Kim L, Scott M, Wu J-J and Eyre DR (2010) Location of 3-hydroxyproline residues in collagen types I, II, III, and V/XI implies a role in fibril supramolecular assembly. *J Biol Chem* **285**, 2580–2590.
27 Hudson DM and Eyre DR (2013) Collagen prolyl 3-hydroxylation: a major role for a minor post-translational modification? *Connect Tissue Res* **54**, 245–251.
28 Fidler AL, Boudko SP, Rokas A and Hudson BG (2018) The triple helix of collagens – an ancient protein structure that enabled animal multicellularity and tissue evolution. *J Cell Sci* **131**, jcs203950.
29 Myllyharju J and Kivirikko KI (2004) Collagens, modifying enzymes and their mutations in humans, flies and worms. *Trends Genet* **20**, 33–43.
30 Prockop DJ, Kivirikko KI, Tuderman L and Guzman NA (1979) The biosynthesis of collagen and its disorders. *N Engl J Med* **301**, 77–85.
31 Canty EG, Lu Y, Meadows RS, Shaw MK, Holmes DF and Kadler KE (2004) Coalignment of plasma membrane channels and protrusions (fibripositors) specifies the parallelism of tendon. *J Cell Biol* **165**, 553–563.
32 Revell CK, Herrera JA, Lawless C, Lu Y, Kadler KE, Chang J and Jensen OE (2023) Modelling collagen fibril self-assembly from extracellular medium in embryonic tendon. *bioRxiv* [PREPRINT]. doi: 10.1101/2023.03.13.532430
33 Salo AM and Myllyharju J (2021) Prolyl and lysyl hydroxylases in collagen synthesis. *Exp Dermatol* **30**, 38–49.
34 Gjaltema RAF and Bank RA (2017) Molecular insights into prolyl and lysyl hydroxylation of fibrillar collagens in health and disease. *Crit Rev Biochem Mol Biol* **52**, 74–95.
35 Xu X, Chiu J, Chen S and Fang C (2021) Pathophysiological roles of cell surface and extracellular protein disulfide isomerase and their molecular mechanisms. *Br J Pharmacol* **178**, 2911–2930.
36 Wang Z and Griffin M (2012) TG2, a novel extracellular protein with multiple functions. *Amino Acids* **42**, 939–949.
37 Kagan HM and Trackman PC (1991) Properties and function of lysyl oxidase. *Am J Respir Cell Mol Biol* **5**, 206–210.
38 Provenzano PP, Eliceiri KW, Yan L, Ada-Nguema A, Conklin MW, Inman DR and Keely PJ (2008) Nonlinear optical imaging of cellular processes in breast cancer. *Microsc Microanal* **14**, 532–548.

18733468, 2024, 6, Downloaded from https://febs.onlinelibrary.wiley.com/doi/10.1002/1873-3468.14852, Wiley Online Library on [30/08/2025]. See the Terms and Conditions (https://onlinelibrary.wiley.com/terms-and-conditions) on Wiley Online Library for rules of use; OA articles are governed by the applicable Creative Commons License

39 Conklin MW, Eickhoff JC, Riching KM, Pehlke CA, Eliceiri KW, Provenzano PP, Friedl A and Keely PJ (2011) Aligned collagen is a prognostic signature for survival in human breast carcinoma. *Am J Pathol* **178**, 1221–1232.

40 Richards AJ and Snead MP (2022) Molecular basis of pathogenic variants in the fibrillar collagens. *Genes* **13**, 1199.

41 Van Doren SR (2015) Matrix metalloproteinase interactions with collagen and elastin. *Matrix Biol* **44**, 224–231.

42 Rydlova M, Holubec L, Ludvikova M, Kalfert D, Franekova J and Povysil C (2008) Biological activity and clinical implications of the matrix metalloproteinases. *Anticancer Res* **28**, 1389–1397.

43 Ray A and Provenzano PP (2021) Aligned forces: origins and mechanisms of cancer dissemination guided by extracellular matrix architecture. *Curr Opin Cell Biol* **72**, 63–71.

44 Angel PM and Zambrzycki SC (2022) Predictive value of collagen in cancer. *Adv Cancer Res* **154**, 15–45.

45 Ouellette JN, Drifka CR, Pointer KB, Liu Y, Lieberthal TJ, Kao WJ, Kuo JS, Loeffler AG and Eliceiri KW (2021) Navigating the collagen jungle: the biomedical potential of fiber organization in cancer. *Bioengineering* **8**, 17.

46 Adams JC (2023) Passing the post: roles of posttranslational modifications in the form and function of extracellular matrix. *Am J Physiol Cell Physiol* **324**, C1179–C1197.

47 Clift CL, Saunders J, Drake RR and Angel PM (2022) Perspectives on pediatric congenital aortic valve stenosis: extracellular matrix proteins, post translational modifications, and proteomic strategies. *Front Cardiovasc Med* **9**, 1024049.

48 Szekeres GP, Pagel K and Heiner Z (2022) Analytical challenges of glycosaminoglycans at biological interfaces. *Anal Bioanal Chem* **414**, 85–93.

49 Pepi LE, Sanderson P, Stickney M and Amster IJ (2021) Developments in mass spectrometry for glycosaminoglycan analysis: a review. *Mol Cell Proteomics* **20**, 100025.

50 Laronha H and Caldeira J (2020) Structure and function of human matrix metalloproteinases. *Cells* **9**, 1076.

51 Naba A (2023) Ten years of extracellular matrix proteomics: accomplishments, challenges, and future perspectives. *Mol Cell Proteomics* **22**, 100528.

52 Naba A, Clauser KR and Hynes RO (2015) Enrichment of extracellular matrix proteins from tissues and digestion into peptides for mass spectrometry analysis. *J Vis Exp* **101**, e53057.

53 Naba A, Pearce OMT, Del Rosario A, Ma D, Ding H, Rajeeve V, Cutillas PR, Balkwill FR and Hynes RO (2017) Characterization of the extracellular matrix of normal and diseased tissues using proteomics. *J Proteome Res* **16**, 3083–3091.

54 Shao X, Taha IN, Clauser KR, Gao Y and Naba A (2020) MatrisomeDB: the ECM-protein knowledge database. *Nucleic Acids Res* **48**, D1136–D1144.

55 Angel PM, Nusinow D, Brown CB, Violette K, Barnett JV, Zhang B, Baldwin HS and Caprioli RM (2011) Networked-based characterization of extracellular matrix proteins from adult mouse pulmonary and aortic valves. *J Proteome Res* **10**, 812–823.

56 Mendibil U, Ruiz-Hernandez R, Retegi-Carrion S, Garcia-Urquia N, Olalde-Graells B and Abarrategi A (2020) Tissue-specific decellularization methods: rationale and strategies to achieve regenerative compounds. *Int J Mol Sci* **21**, 5447.

57 Choudhury D, Yee M, Sheng ZLJ, Amirul A and Naing MW (2020) Decellularization systems and devices: state-of-the-art. *Acta Biomater* **115**, 51–59.

58 Biehl A, Martins AMG, Davis ZG, Sze D, Collins L, Mora-Navarro C, Fisher MB and Freytes DO (2023) Towards a standardized multi-tissue decellularization protocol for the derivation of extracellular matrix materials. *Biomater Sci* **11**, 641–654.

59 Chen WC, Wang Z, Missinato MA, Park DW, Long DW, Liu HJ, Zeng X, Yates NA, Kim K and Wang Y (2016) Decellularized zebrafish cardiac extracellular matrix induces mammalian heart regeneration. *Sci Adv* **2**, e1600844.

60 Didangelos A, Yin X, Mandal K, Baumert M, Jahangiri M and Mayr M (2010) Proteomics characterization of extracellular space components in the human aorta. *Mol Cell Proteomics* **9**, 2048–2062.

61 Garcia-Puig A, Mosquera JL, Jimenez-Delgado S, Garcia-Pastor C, Jorba I, Navajas D, Canals F and Raya A (2019) Proteomics analysis of extracellular matrix remodeling during zebrafish heart regeneration. *Mol Cell Proteomics* **18**, 1745–1755.

62 Sonpho E, Mann FG Jr, Levy M, Ross EJ, Guerrero-Hernandez C, Florens L, Saraf A, Doddihal V, Ounjai P and Sanchez Alvarado A (2021) Decellularization enables characterization and functional analysis of extracellular matrix in planarian regeneration. *Mol Cell Proteomics* **20**, 100137.

63 Carpino G, Overi D, Melandro F, Grimaldi A, Cardinale V, Di Matteo S, Mennini G, Rossi M, Alvaro D, Barnaba V *et al.* (2019) Matrisome analysis of intrahepatic cholangiocarcinoma unveils a peculiar cancer-associated extracellular matrix structure. *Clin Proteomics* **16**, 37.

64 Schiller HB, Fernandez IE, Burgstaller G, Schaab C, Scheltema RA, Schwarzmayr T, Strom TM, Eickelberg O and Mann M (2015) Time- and compartment-resolved proteome profiling of the extracellular niche in lung injury and repair. *Mol Syst Biol* **11**, 819.

18733468, 2024, 6, Downloaded from https://febs.onlinelibrary.wiley.com/doi/10.1002/1873-3468.14852, Wiley Online Library on [30/08/2025]. See the Terms and Conditions (https://onlinelibrary.wiley.com/terms-and-conditions) on Wiley Online Library for rules of use; OA articles are governed by the applicable Creative Commons License

65 Naba A, Clauser KR, Hoersch S, Liu H, Carr SA and Hynes RO (2012) The matrisome: in silico definition and in vivo characterization by proteomics of normal and tumor extracellular matrices. *Mol Cell Proteomics* **11**, M111.014647.
66 Clift CL, Su YR, Bichell D, Smith HCJ, Bethard JR, Norris-Caneda K, Comte-Walters S, Ball LE, Hollingsworth MA, Mehta AS *et al.* (2021) Collagen fiber regulation in human pediatric aortic valve development and disease. *Sci Rep* **11**, 1–17.
67 Wilson R, Diseberg AF, Gordon L, Zivkovic S, Tatarczuch L, Mackie EJ, Gorman JJ and Bateman JF (2010) Comprehensive profiling of cartilage extracellular matrix formation and maturation using sequential extraction and label-free quantitative proteomics. *Mol Cell Proteomics* **9**, 1296–1313.
68 Angel PM, Comte-Walters S, Ball LE, Talbot K, Brockbank KGM, Mehta AS and Drake RR (2018) Mapping extracellular matrix proteins in formalin-fixed, paraffin-embedded tissues by MALDI imaging mass spectrometry. *J Proteome Res* **17**, 635–646.
69 Macdonald JK, Clift CL, Saunders J, Zambrzycki SC, Mehta AS, Drake RR and Angel PM (2024) Differential protease specificity by collagenase as a novel approach to serum proteomics that includes identification of extracellular matrix proteins without enrichment. *J Am Soc Mass Spectrom* **35**, 487–497.
70 Barrett AS, Wither MJ, Hill RC, Dzieciatkowska M, D'Alessandro A, Reisz JA and Hansen KC (2017) Hydroxylamine chemical digestion for insoluble extracellular matrix characterization. *J Proteome Res* **16**, 4177–4184.
71 Keil B (1962) The chemistry of peptides and proteins. *Annu Rev Biochem* **31**, 139–172.
72 Li J, Ma J, Zhang Q, Gong H, Gao D, Wang Y, Li B, Li X, Zheng H and Wu Z (2022) Spatially resolved proteomic map shows that extracellular matrix regulates epidermal growth. *Nat Commun* **13**, 4012.
73 Eckhard U, Huesgen PF, Brandstetter H and Overall CM (2014) Proteomic protease specificity profiling of clostridial collagenases reveals their intrinsic nature as dedicated degraders of collagen. *J Proteomics* **100**, 102–114.
74 Krasny L, Bland P, Kogata N, Wai P, Howard BA, Natrajan RC and Huang PH (2018) SWATH mass spectrometry as a tool for quantitative profiling of the matrisome. *J Proteomics* **189**, 11–22.
75 Hebert JD, Myers SA, Naba A, Abbruzzese G, Lamar JM, Carr SA and Hynes RO (2020) Proteomic profiling of the ECM of xenograft breast cancer metastases in different organs reveals distinct metastatic niches. *Cancer Res* **80**, 1475–1485.
76 Naba A, Clauser KR, Mani DR, Carr SA and Hynes RO (2017) Quantitative proteomic profiling of the extracellular matrix of pancreatic islets during the angiogenic switch and insulinoma progression. *Sci Rep* **7**, 40495.
77 Thorsen A-SF, Riber LPS, Rasmussen LM and Overgaard M (2023) A targeted multiplex mass spectrometry method for quantitation of abundant matrix and cellular proteins in formalin-fixed paraffin embedded arterial tissue. *J Proteomics* **272**, 104775.
78 Kirkpatrick DS, Gerber SA and Gygi SP (2005) The absolute quantification strategy: a general procedure for the quantification of proteins and post-translational modifications. *Methods* **35**, 265–273.
79 Goddard ET, Hill RC, Barrett A, Betts C, Guo Q, Maller O, Borges VF, Hansen KC and Schedin P (2016) Quantitative extracellular matrix proteomics to study mammary and liver tissue microenvironments. *Int J Biochem Cell Biol* **81**, 223–232.
80 McCabe MC, Hill RC, Calderone K, Cui Y, Yan Y, Quan T, Fisher GJ and Hansen KC (2020) Alterations in extracellular matrix composition during aging and photoaging of the skin. *Matrix Biol Plus* **8**, 100041.
81 Shao X, Gomez CD, Kapoor N, Considine JM, Grams C, Gao Y and Naba A (2023) MatrisomeDB 2.0: 2023 updates to the ECM-protein knowledge database. *Nucleic Acids Res* **51**, D1519–D1530.
82 Petrov PB, Considine JM, Izzi V and Naba A (2023) Matrisome AnalyzeR: a suite of tools to annotate and quantify ECM molecules in big datasets across organisms. *bioRxiv* [PREPRINT]. doi: 10.1101/2023.04.18.537378
83 Wissowzky A (1876) Ueber das eosin als reagenz auf Hämoglobin und die Bildung von Blutgefässen und Blutkörperchen bei Säugetier und Hühnerembryonen (about eosin as a reagent for hemoglobin and the formation of blood vessels and blood cells in mammals and chicken embryos). *Arch Mikrosk Anat* **13**, 479–496.
84 Titford M (2005) The long history of hematoxylin. *Biotech Histochem* **80**, 73–78.
85 Ortiz-Hidalgo C and Pina-Oviedo S (2019) Hematoxylin: Mesoamerica's gift to histopathology. Palo de Campeche (logwood tree), Pirates' most desired treasure, and irreplaceable tissue stain. *Int J Surg Pathol* **27**, 4–14.
86 Chan JK (2014) The wonderful colors of the hematoxylin-eosin stain in diagnostic surgical pathology. *Int J Surg Pathol* **22**, 12–32.
87 Lillie RD and Pizzolato P (1972) Mechanisms of iron II and iron 3 sequence hematoxylin stains. *J Histochem Cytochem* **20**, 13–129.
88 Titford M (2013) Progress in the development of microscopical techniques for diagnostic pathology. *J Histotechnol* **32**, 9–19.
89 Monaghan MG, Kroll S, Brucker SY and Schenke-Layland K (2016) Enabling multiphoton and second harmonic generation imaging in paraffin-embedded

18733468, 2024, 6, Downloaded from https://febs.onlinelibrary.wiley.com/doi/10.1002/1873-3468.14852, Wiley Online Library on [30/08/2025]. See the Terms and Conditions (https://onlinelibrary.wiley.com/terms-and-conditions) on Wiley Online Library for rules of use; OA articles are governed by the applicable Creative Commons License

and histologically stained sections. *Tissue Eng Part C Methods* **22**, 517–523.
90 Masson P (1929) Some histological methods; trichrome stainings and their preliminary technique. *J Tech Methods* **12**, 15.
91 Goldner J (1937) A modification of the Masson trichrome technique for routine laboratory purposes. *Am J Pathol* **14**, 237–243.
92 Buk S (1984) Simultaneous demonstration of connective tissue elastica and fibrin by a combined Verhoeff's elastic-Martius-scarlet-blue trichrome stain. *Stain Technol* **59**, 1–5.
93 Pastore GN, Dicola LP, Norman DR and Gardner RM (1992) Effect of estriol on the structure and organization of collagen in the lamina propria of the immature rat uterus. *Biol Reprod* **47**, 83–91.
94 Yi ES, Lee H, Yin S, Piguet P, Sarosi I, Kaufmann S, Tarpley J, Wang N-S and Ulich TR (1996) Platelet-derived growth factor causes pulmonary cell proliferation and collagen deposition in vivo. *Am J Pathol* **149**, 539–548.
95 Mao H, Su P, Qiu W, Huang L, Yu H and Wang Y (2016) The use of Masson's trichrome staining, second harmonic imaging and two-photon excited fluorescence of collagen in distinguishing intestinal tuberculosis from Crohn's disease. *Colorectal Dis* **18**, 6–1178.
96 Baidoo N, Sanger GJ and Belai A (2023) Histochemical and biochemical analysis of collagen content in formalin-fixed, paraffin embedded colonic samples. *MethodsX* **11**, 102416.
97 Pires LAS, Fosse AM Jr, Ribeiro JGA, Postigo PRM, Manaia JHM and Babinski MA (2023) Stereological comparison of smooth muscle, collagen, and elastic fibers of the clitoris and glans penis in young adults. *Morphologie* **108**, 100721.
98 Angel PM, Drake RR, Park Y, Clift CL, West C, Berkhiser S, Hardiman G, Mehta AS, Bichell DP and Su YR (2021) Spatial N-glycomics of the human aortic valve in development and pediatric endstage congenital aortic valve stenosis. *J Mol Cell Cardiol* **154**, 6–20.
99 Edston E and Gröntoft L (1997) A connective tissue counterstain in routine pathology. *J Histotechnol* **20**, 123–125.
100 Ceccopieri C, Skonieczna J and Madej JP (2021) Modification of a haematoxylin, eosin, and natural saffron staining method for the detection of connective tissue. *J Vet Res* **65**, 125–130.
101 Fitzgerald A (1953) Haemalum, phloxine, saffron as a routine stain. *Can J Med Technol* **15**, 145–149.
102 Putten LV and Zweiten MV (1988) Studies on prolactin-secreting cells in aging rats of different strains. *Mech Ageing Dev* **42**, 12.
103 Movat HZ (1955) Demonstration of all connective tissue elements in a single section; pentachrome stains. *AMA Arch Pathol* **60**, 289–295.
104 Stephens EH, Post AD, Laucirica DR and Grande-Allen KJ (2010) Perinatal changes in mitral and aortic valve structure and composition. *Pediatr Dev Pathol* **13**, 447–458.
105 Herovici C (1963) Picropolychrome: histological staining technic intended for the study of normal and pathological connective tissue. *Rev Fr Etud Clin Biol* **8**, 88–89.
106 Levame M and Meyer F (1987) Herovici's picropolychromium. Application to the identification of type I and III collagens. *Pathol Biol* **35**, 1183–1188.
107 Turner NJ, Pezzone MA, Brown B and Badylak S (2013) Quantitative multispectral imaging of Herovici's polychrome for the assessment of collagen content and tissue remodelling. *J Tissue Eng Regen Med* **7**, 139–148.
108 Su CY, Liu TY, Wang HV and Yang WC (2023) Histopathological study on collagen in full-thickness wound healing in Fraser's dolphins (*Lagenodelphis hosei*). *Animals (Basel)* **13**, 1681.
109 Rawlins JM, Lam WL, Karoo RO, Naylor IL and Sharpe DT (2006) Quantifying collagen type in mature burn scars: a novel approach using histology and digital image analysis. *J Burn Care Res* **27**, 60–65.
110 Ozog DM, Liu A, Chaffins ML, Ormsby AH, Fincher EF, Chipps LK, Mi Q-S, Grossman PH, Pui JC and Moy RL (2013) Evaluation of clinical results, histological architecture, and collagen expression following treatment of mature burn scars with a fractional carbon dioxide laser. *JAMA Dermatol* **149**, 50–57.
111 Teuscher AC, Statzer C, Pantasis S, Bordoli MR and Ewald CY (2019) Assessing collagen deposition during aging in mammalian tissue and in *Caenorhabditis elegans*. *Methods Mol Biol* **1944**, 169–188.
112 Widgerow AD and Napekoski K (2021) New approaches to skin photodamage histology-differentiating 'good' versus 'bad' elastin. *J Cosmet Dermatol* **20**, 526–531.
113 Weerakoon AT, Condon N, Cox TR, Sexton C, Cooper C, Meyers IA, Thomson D, Ford PJ, Roy S and Symons AL (2022) Dynamic dentin: a quantitative microscopic assessment of age and spatial changes to matrix architecture, peritubular dentin, and collagens types I and III. *J Struct Biol* **214**, 107899.
114 Sweat F, Puchtler H and Rosenthal CI (1964) Sirius red F3BA as a stain for connective tissue. *Arch Pathol* **78**, 69–72.
115 Nielsen LF, Moe D, Kirkeby S and Garbarsch C (1998) Sirius red and acid fuchsin staining mechanisms. *Biotech Histochem* **73**, 71–77.
116 Constantine VS and Mowry RW (1968) Selective staining of human dermal collagen. *J Invest Dermatol* **50**, 419–423.
117 Padilla CMLPD, Coenen MJ, Tovar A, Vega REDL, Evans CH and Müller SA (2021) Picrosirius red staining: revisiting its application to the qualitative

18733468, 2024, 6, Downloaded from https://febs.onlinelibrary.wiley.com/doi/10.1002/1873-3468.14852, Wiley Online Library on [30/08/2025]. See the Terms and Conditions (https://onlinelibrary.wiley.com/terms-and-conditions) on Wiley Online Library for rules of use; OA articles are governed by the applicable Creative Commons License

and quantitative assessment of collagen type I and type III in tendon. *J Histochem Cytochem* **69**, 633–643.
118 Fine S and Hansen WP (1971) Optical second harmonic generation in biological systems. *Appl Optics* **10**, 2350–2353.
119 Changoor A, Nelea M, Methot S, Tran-Khanh N, Chevrier A, Restrepo A, Shive MS, Hoemann CD and Buschmann MD (2011) Structural characteristics of the collagen network in human normal, degraded and repair articular cartilages observed in polarized light and scanning electron microscopies. *Osteoarthr Cartil* **19**, 1458–1468.
120 Hoogenboom BW (2021) Stretching the resolution limit of atomic force microscopy. *Nat Struct Mol Biol* **28**, 629–630.
121 Calò A, Romin Y, Srouji R, Zambirinis CP, Fan N, Santella A, Feng E, Fujisawa S, Turkekul M and Huang S (2020) Spatial mapping of the collagen distribution in human and mouse tissues by force volume atomic force microscopy. *Sci Rep* **10**, 15664.
122 Egerton RF (2008) Physical Principles of Electron Microscopy. 1st edn. Springer Verlag, New York, NY.
123 Fischer E, Hansen B, Nair V, Hoyt FH and Dorward D (2012) Scanning electron microscopy. *Curr Protoc Microbiol* **Chapter 2**, Unit 2B.2.
124 Shih C-C, Oakley DM, Joens MS, Roth RA and Fitzpatrick JAJ (2018) Nonlinear optical imaging of extracellular matrix proteins. *Methods Cell Biol* **143**, 57–78.
125 Tilbury K and Campagnola PJ (2015) Applications of second-harmonic generation imaging microscopy in ovarian and breast cancer. *Perspect Medicin Chem* **7**, 21–32.
126 Chen X, Nadiarynkh O, Plotnikov S and Campagnola PJ (2012) Second harmonic generation microscopy for quantitative analysis of collagen fibrillar structure. *Nat Protoc* **7**, 654.
127 Yeh CH, Tan CZ, Cheng CA, Hung JT and Chen SY (2018) Improving resolution of second harmonic generation microscopy via scanning structured illumination. *Biomed Opt Express* **9**, 6081–6090.
128 Xi G, Guo W, Kang D, Ma J, Fu F, Qiu L, Zheng L, He J, Fang N, Chen J *et al.* (2021) Large-scale tumor-associated collagen signatures identify high-risk breast cancer patients. *Theranostics* **11**, 3229–3243.
129 Li B, Nelson MS, Savari O, Loeffler AG and Eliceiri KW (2022) Differentiation of pancreatic ductal adenocarcinoma and chronic pancreatitis using graph neural networks on histopathology and collagen fiber features. *J Pathol Inform* **13**, 100158.
130 Huang X, Fu F, Guo W, Kang D, Han X, Zheng L, Zhan Z, Wang C, Zhang Q, Wang S *et al.* (2023) Prognostic significance of collagen signatures at breast tumor boundary obtained by combining multiphoton imaging and imaging analysis. *Cell Oncol (Dordr)* **47**, 69–80.
131 Femino AM, Fay FS, Fogarty K and Singer RH (1998) Visualization of single RNA transcripts in situ. *Science* **280**, 585–590.
132 Ståhl PL, Salmén F, Vickovic S, Lundmark A, Navarro JF, Magnusson J, Giacomello S, Asp M, Westholm JO and Huss M (2016) Visualization and analysis of gene expression in tissue sections by spatial transcriptomics. *Science* **353**, 78–82.
133 Bingham GC, Lee F, Naba A and Barker TH (2020) Spatial-omics: novel approaches to probe cell heterogeneity and extracellular matrix biology. *Matrix Biol* **91-92**, 152–166.
134 Merritt CR, Ong GT, Church SE, Barker K, Danaher P, Geiss G, Hoang M, Jung J, Liang Y and McKay-Fleisch J (2020) Multiplex digital spatial profiling of proteins and RNA in fixed tissue. *Nat Biotechnol* **38**, 586–599.
135 Moses L and Pachter L (2022) Museum of spatial transcriptomics. *Nat Methods* **19**, 534–546.
136 Van TM and Blank CU (2019) A user's perspective on GeoMxTM digital spatial profiling. *Immunooncol Technol* **1**, 11–18.
137 Wang N, Li X, Wang R and Ding Z (2021) Spatial transcriptomics and proteomics technologies for deconvoluting the tumor microenvironment. *Biotechnol J* **16**, e2100041.
138 Nielsen SH, Mouton AJ, DeLeon-Pennell KY, Genovese F, Karsdal M and Lindsey ML (2019) Understanding cardiac extracellular matrix remodeling to develop biomarkers of myocardial infarction outcomes. *Matrix Biol* **75–76**, 43–57.
139 Mund A, Brunner A-D and Mann M (2022) Unbiased spatial proteomics with single-cell resolution in tissues. *Mol Cell* **82**, 2335–2349.
140 Wiza JL (1979) Microchannel plate detectors. *Nucl Instrum Methods* **162**, 587–601.
141 Jungmann JH and Heeren RMA (2013) Detection systems for mass spectrometry imaging: a perspective on novel developments with a focus on active pixel detectors. *Rapid Commun Mass Spectrom* **27**, 1–23.
142 Giesen C, Wang HAO, Schapiro D, Zivanovic N, Jacobs A, Hattendorf B, Schüffler PJ, Grolimund D, Buhmann JM and Brandt S (2014) Highly multiplexed imaging of tumor tissues with subcellular resolution by mass cytometry. *Nat Methods* **11**, 417–422.
143 Bandura DR, Baranov VI, Ornatsky OI, Antonov A, Kinach R, Lou X, Pavlov S, Vorobiev S, Dick JE and Tanner SD (2009) Mass cytometry: technique for real time single cell multitarget immunoassay based on inductively coupled plasma time-of-flight mass spectrometry. *Anal Chem* **81**, 6813–6822.
144 Angelo M, Bendall SC, Finck R, Hale MB, Hitzman C, Borowsky AD, Levenson RM, Lowe JB, Liu SD

18733468, 2024, 6, Downloaded from https://febs.onlinelibrary.wiley.com/doi/10.1002/1873-3468.14852, Wiley Online Library on [30/08/2025]. See the Terms and Conditions (https://onlinelibrary.wiley.com/terms-and-conditions) on Wiley Online Library for rules of use; OA articles are governed by the applicable Creative Commons License

and Zhao S (2014) Multiplexed ion beam imaging of human breast tumors. *Nat Med* **20**, 436–442.
145 Levenson RM, Borowsky AD and Angelo M (2015) Immunohistochemistry and mass spectrometry for highly multiplexed cellular molecular imaging. *Lab Invest* **95**, 397–405.
146 Keren L, Bosse M, Thompson S, Risom T, Vijayaragavan K, McCaffrey E, Marquez D, Angoshtari R, Greenwald NF and Fienberg H (2019) MIBI-TOF: a multiplexed imaging platform relates cellular phenotypes and tissue structure. *Sci Adv* **5**, eaax5851.
147 Yagnik G, Liu Z, Rothschild KJ and Lim MJ (2021) Highly multiplexed immunohistochemical MALDI-MS imaging of biomarkers in tissues. *J Am Soc Mass Spectrom* **32**, 977–988.
148 Claes BSR, Krestensen KK, Yagnik G, Grgic A, Kuik C, Lim MJ, Rothschild KJ, Vandenbosch M and Heeren RMA (2023) MALDI-IHC-guided in-depth spatial proteomics: targeted and untargeted MSI combined. *Anal Chem* **95**, 2329–2338.
149 Simone NL, Bonner RF, Gillespie JW, Emmert-Buck MR and Liotta LA (1998) Laser-capture microdissection: opening the microscopic frontier to molecular analysis. *Trends Genet* **14**, 272–276.
150 Chen Y, Gote-Schniering J, Müller M, Albanese P, Jankevics A, Jentzsch RC, Tata A, Ansari M, De Sadeleer L and Yang L (2023) A spatially resolved extracellular matrix proteome atlas of the distal human lung. ERS International Congress 2023 abstracts. 10.1183/13993003.congress-2023.OA2626
151 Galle P, Hamburger J and Castaing R (1970) Sur une nouvelle méthode d'analyse cellulaire utilisant le phénomène d'émission ionique secondaire. *Ann Phys Biol Med* **42**, 83–94.
152 Caprioli RM, Farmer TB and Gile J (1997) Molecular imaging of biological samples: localization of peptides and proteins using MALDI-TOF MS. *Anal Chem* **69**, 4751–4760.
153 Colliver TL, Brummel CL, Pacholski ML, Swanek FD, Ewing AG and Winograd N (1997) Atomic and molecular imaging at the single-cell level with TOF-SIMS. *Anal Chem* **69**, 2225–2231.
154 Krestensen KK, Heeren RMA and Balluff B (2023) State-of-the-art mass spectrometry imaging applications in biomedical research. *Analyst* **148**, 6161–6187.
155 Moore JL and Charkoftaki G (2023) A guide to MALDI imaging mass spectrometry for tissues. *J Proteome Res* **22**, 3401–3417.
156 Norris JL and Caprioli RM (2013) Analysis of tissue specimens by matrix-assisted laser desorption/ionization imaging mass spectrometry in biological and clinical research. *Chem Rev* **113**, 2309–2342.
157 Misevic GN, Rasser B, Norris V, Dérue C, Gibouin D, Lefebvre F, Verdus MC, Delaune A, Legent G and Ripoll C (2009) Chemical microscopy of biological samples by dynamic mode secondary ion mass spectrometry. *Methods Mol Biol* **522**, 163–173.
158 Mellinger AL, Garrard KP, Khodjaniyazova S, Rabbani ZN, Gamcsik MP and Muddiman DC (2022) Multiple infusion start time mass spectrometry imaging of dynamic SIL-glutathione biosynthesis using infrared matrix-assisted laser desorption electrospray ionization. *J Proteome Res* **21**, 747–757.
159 Fideler J, Johanningsmeier SD, Ekelof M and Muddiman DC (2019) Discovery and quantification of bioactive peptides in fermented cucumber by direct analysis IR-MALDESI mass spectrometry and LC-QQQ-MS. *Food Chem* **271**, 715–723.
160 Pace CL, Angel PM, Drake RR and Muddiman DC (2022) Mass spectrometry imaging of N-linked glycans in a formalin-fixed paraffin-embedded human prostate by infrared matrix-assisted laser desorption electrospray ionization. *J Proteome Res* **21**, 243–249.
161 Cournut A, Moustiez P, Coffinier Y, Enjalbal C and Bich C (2023) Innovative SALDI mass spectrometry analysis for Alzheimer's disease synthetic peptides detection. *Talanta* **268**, 125357.
162 Cournut A, Hosu IS, Braud F, Moustiez P, Coffinier Y, Enjalbal C and Bich C (2023) Development of nanomaterial enabling highly sensitive surface-assisted laser desorption/ionization mass spectrometry peptide analysis. *Rapid Commun Mass Spectrom* **37**, e9476.
163 Wong KFC, Greatorex RE, Gidman CE, Rahman S and Griffiths RL (2023) Surface-sampling mass spectrometry to study proteins and protein complexes. *Essays Biochem* **67**, 229–241.
164 Towers MW, Karancsi T, Jones EA, Pringle SD and Claude E (2018) Optimised desorption electrospray ionisation mass spectrometry imaging (DESI-MSI) for the analysis of proteins/peptides directly from tissue sections on a travelling wave ion mobility Q-ToF. *J Am Soc Mass Spectrom* **29**, 2456–2466.
165 Garza KY, Feider CL, Klein DR, Rosenberg JA, Brodbelt JS and Eberlin LS (2018) Desorption electrospray ionization mass spectrometry imaging of proteins directly from biological tissue sections. *Anal Chem* **90**, 7785–7789.
166 Hsu CC, Chou PT and Zare RN (2015) Imaging of proteins in tissue samples using nanospray desorption electrospray ionization mass spectrometry. *Anal Chem* **87**, 11171–11175.
167 Chen CL, Kuo TH, Chung HH, Huang P, Lin LE and Hsu CC (2021) Remodeling nanoDESI platform with ion mobility spectrometry to expand protein coverage in cancerous tissue. *J Am Soc Mass Spectrom* **32**, 653–660.
168 Hale OJ and Cooper HJ (2021) Native mass spectrometry imaging of proteins and protein complexes by Nano-DESI. *Anal Chem* **93**, 4619–4627.

18733468, 2024, 6, Downloaded from https://febs.onlinelibrary.wiley.com/doi/10.1002/1873-3468.14852, Wiley Online Library on [30/08/2025]. See the Terms and Conditions (https://onlinelibrary.wiley.com/terms-and-conditions) on Wiley Online Library for rules of use; OA articles are governed by the applicable Creative Commons License

169 Hale OJ, Hughes JW, Sisley EK and Cooper HJ (2022) Native ambient mass spectrometry enables analysis of intact endogenous protein assemblies up to 145 kDa directly from tissue. *Anal Chem* **94**, 5608–5614.
170 Kiss A, Smith DF, Reschke BR, Powell MJ and Heeren RM (2014) Top-down mass spectrometry imaging of intact proteins by laser ablation ESI FT-ICR MS. *Proteomics* **14**, 1283–1289.
171 Buchberger AR, DeLaney K, Johnson J and Li L (2018) Mass spectrometry imaging: a review of emerging advancements and future insights. *Anal Chem* **90**, 240–265.
172 Groseclose MR, Andersson M, Hardesty WM and Caprioli RM (2007) Identification of proteins directly from tissue: in situ tryptic digestions coupled with imaging mass spectrometry. *J Mass Spectrom* **42**, 254–262.
173 Angel PM, Norris-Caneda K and Drake RR (2018) Icptides by MALDI imaging mass spectrometry using fresh-frozen or formalin-fixed, paraffin-embedded tissue. *Curr Protoc Protein Sci* **94**, e65.
174 Ronci M, Bonanno E, Colantoni A, Pieroni L, Di Ilio C, Spagnoli LG, Federici G and Urbani A (2008) Protein unlocking procedures of formalin-fixed paraffin-embedded tissues: application to MALDI-TOF imaging MS investigations. *Proteomics* **8**, 3702–3714.
175 Casadonte R and Caprioli RM (2011) Proteomic analysis of formalin-fixed paraffin-embedded tissue by MALDI imaging mass spectrometry. *Nat Protoc* **6**, 1695–1709.
176 Boyle ST, Mittal P, Kaur G, Hoffmann P, Samuel MS and Klingler-Hoffmann M (2020) Uncovering tumor-stroma inter-relationships using MALDI mass spectrometry imaging. *J Proteome Res* **19**, 4093–4103.
177 Buerger M, Klein O, Kapahnke S, Mueller V, Frese JP, Omran S, Greiner A, Sommerfeld M, Kaschina E, Jannasch A *et al.* (2021) Use of MALDI mass spectrometry imaging to identify proteomic signatures in aortic aneurysms after endovascular repair. *Biomedicines* **9**, 1088.
178 Phillips L, Gill AJ and Baxter RC (2019) Novel prognostic markers in triple-negative breast cancer discovered by MALDI-mass spectrometry imaging. *Front Oncol* **9**, 379.
179 Baltzer AW, Casadonte R, Korff A, Baltzer LM, Kriegsmann K, Kriegsmann M and Kriegsmann J (2023) Biological injection therapy with leukocyte-poor platelet-rich plasma induces cellular alterations, enhancement of lubricin, and inflammatory downregulation in vivo in human knees: a controlled, prospective human clinical trial based on mass spectrometry imaging analysis. *Front Surg* **10**, 1169112.
180 Angel PM, Bruner E, Bethard J, Clift CL, Ball L, Drake RR and Feghali-Bostwick C (2020) Extracellular matrix alterations in low-grade lung adenocarcinoma compared with normal lung tissue by imaging mass spectrometry. *J Mass Spectrom* **55**, e4450.
181 Angel PM, Schwamborn K, Comte-Walters S, Clift CL, Ball LE, Mehta AS and Drake RR (2019) Extracellular matrix imaging of breast tissue pathologies by MALDI-imaging mass spectrometry. *Proteomics Clin Appl* **13**, e1700152.
182 Arolt C, Hoffmann F, Nachtsheim L, Wolber P, Guntinas-Lichius O, Buettner R, von Eggeling F, Quaas A and Klussmann JP (2022) Mutually exclusive expression of COL11A1 by CAFs and tumour cells in a large panCancer and a salivary gland carcinoma cohort. *Head Neck Pathol* **16**, 394–406.
183 Arolt C, Meyer M, Hoffmann F, Wagener-Ryczek S, Schwarz D, Nachtsheim L, Beutner D, Odenthal M, Guntinas-Lichius O, Buettner R *et al.* (2020) Expression profiling of extracellular matrix genes reveals global and entity-specific characteristics in adenoid cystic, mucoepidermoid and salivary duct carcinomas. *Cancers (Basel)* **12**, 2466.
184 Deininger SO, Bollwein C, Casadonte R, Wandernoth P, Goncalves JPL, Kriegsmann K, Kriegsmann M, Boskamp T, Kriegsmann J, Weichert W *et al.* (2022) Multicenter evaluation of tissue classification by matrix-assisted laser desorption/ionization mass spectrometry imaging. *Anal Chem* **94**, 8194–8201.
185 Longuespee R, Kriegsmann K, Cremer M, Zgorzelski C, Casadonte R, Kazdal D, Kriegsmann J, Weichert W, Schwamborn K, Fresnais M *et al.* (2019) In MALDI-mass spectrometry imaging on formalin-fixed paraffin-embedded tissue specimen section thickness significantly influences m/z peak intensity. *Proteomics Clin Appl* **13**, e1800074.
186 Gessel M, Spraggins JM, Voziyan P, Hudson BG and Caprioli RM (2015) Decellularization of intact tissue enables MALDI imaging mass spectrometry analysis of the extracellular matrix. *J Mass Spectrom* **50**, 1288–1293.
187 Andrews WT, Bickner AN, Tobias F, Ryan KA, Bruening ML and Hummon AB (2021) Electroblotting through enzymatic membranes to enhance molecular tissue imaging. *J Am Soc Mass Spectrom* **32**, 1689–1699.
188 Enthaler B, Trusch M, Fischer M, Rapp C, Pruns JK and Vietzke J-P (2013) MALDI imaging in human skin tissue sections: focus on various matrices and enzymes. *Anal Bioanal Chem* **405**, 1159–1170.
189 Powers TW, Jones EE, Betesh LR, Romano PR, Gao P, Copland JA, Mehta AS and Drake RR (2013) Matrix assisted laser desorption ionization imaging mass spectrometry workflow for spatial profiling

18733468, 2024, 6, Downloaded from https://febs.onlinelibrary.wiley.com/doi/10.1002/1873-3468.14852, Wiley Online Library on [30/08/2025]. See the Terms and Conditions (https://onlinelibrary.wiley.com/terms-and-conditions) on Wiley Online Library for rules of use; OA articles are governed by the applicable Creative Commons License

analysis of N-linked glycan expression in tissues. *Anal Chem* **85**, 9799–9806.
190 West CA, Drake RR and Mehta AS (2020) Enzymatic approach to distinguish Fucosylation isomers of N-linked glycans in tissues using MALDI imaging mass spectrometry. *J Proteome Res* **19**, 2989–2996.
191 Clift CL, Drake RR, Mehta A and Angel PM (2021) Multiplexed imaging mass spectrometry of the extracellular matrix using serial enzyme digests from formalin-fixed paraffin-embedded tissue sections. *Anal Bioanal Chem* **413**, 2709–2719.
192 Sun RC, Young LEA, Bruntz RC, Markussen KH, Zhou Z, Conroy LR, Hawkinson TR, Clarke HA, Stanback AE and Macedo JKA (2021) Brain glycogen serves as a critical glucosamine cache required for protein glycosylation. *Cell Metab* **33**, 1404–1417.
193 Simon HJ, van Agthoven MA, Lam PY, Floris F, Chiron L, Delsuc MA, Rolando C, Barrow MP and O'Connor PB (2016) Uncoiling collagen: a multidimensional mass spectrometry study. *Analyst* **141**, 157–165.
194 Clift CL, Mehta AS, Drake RR and Angel PM (2021) Multiplexed imaging mass spectrometry of histological staining, N-glycan and extracellular matrix from one tissue section: a tool for fibrosis research. *Methods Mol Biol* **2350**, 313–329.
195 Ronci M, Sharma S, Chataway T, Burdon KP, Martin S, Craig JE and Voelcker NH (2011) MALDI-MS-imaging of whole human lens capsule. *J Proteome Res* **10**, 3522–3529.
196 Rujchanarong D, Lefler J, Saunders JE, Pippin S, Spruill L, Bethard JR, Ball LE, Mehta AS, Drake RR, Ostrowski MC *et al.* (2021) Defining the tumor microenvironment by integration of immunohistochemistry and extracellular matrix targeted imaging mass spectrometry. *Cancers (Basel)* **13**, 4419.
197 Clift CL, McLaughlin S, Munoz M, Suuronen EJ, Rotstein BH, Mehta AS, Drake RR, Alarcon EI and Angel PM (2021) Evaluation of therapeutic collagen-based biomaterials in the infarcted mouse heart by extracellular matrix targeted MALDI imaging mass spectrometry. *J Am Soc Mass Spectrom* **32**, 2746–2754.
198 Angel PM, Spruill L, Jefferson M, Bethard JR, Ball LE, Hughes-Halbert C and Drake RR (2020) Zonal regulation of collagen-type proteins and posttranslational modifications in prostatic benign and cancer tissues by imaging mass spectrometry. *Prostate* **80**, 1071–1086.
199 McDowell CT, Klamer Z, Hall J, West CA, Wisniewski L, Powers TW, Angel PM, Mehta AS, Lewin DN and Haab BB (2020) Imaging mass spectrometry and lectin analysis of N-linked glycans in carbohydrate antigen defined pancreatic cancer tissues. *Mol Cell Proteomics* **20**, 100012.
200 Heijs B, Holst S, Briaire-de Bruijn IH, van Pelt GW, de Ru AH, van Veelen PA, Drake RR, Mehta AS, Mesker WE and Tollenaar RA (2016) Multimodal mass spectrometry imaging of N-glycans and proteins from the same tissue section. *Anal Chem* **88**, 7745–7753.
201 Clift C, Drake RR, Mehta AS and Angel PM (2018) Comparative 2D N-glycome, stromal peptide, and tryptic peptide mapping from the same FFPE tissue section using MALDI imaging mass spectrometry. In Second Annual Imaging MAss Spectrometry Conference, Charleston, SC (Presentation P, ed.).
202 Angel PM, Mehta A, Norris-Caneda K and Drake RR (2018) MALDI imaging mass spectrometry of N-glycans and tryptic peptides from the same formalin-fixed, paraffin-embedded tissue section. In Tissue Proteomics: Methods and Protocols (Sarwal MM and Sigdel TK, eds), pp. 225–241. Springer, New York, NY.
203 Seeley EH, Liu Z, Yuan S, Stroope C, Cockerham E, Rashdan NA, Delgadillo LF, Finney AC, Kumar D and Das S (2023) Spatially resolved metabolites in stable and unstable human atherosclerotic plaques identified by mass spectrometry imaging. *Arterioscler Thromb Vasc Biol* **43**, 1626–1635.
204 Mondon P, Hillion M, Peschard O, Andre N, Marchand T, Doridot E, Feuilloley MG, Pionneau C and Chardonnet S (2015) Evaluation of dermal extracellular matrix and epidermal-dermal junction modifications using matrix-assisted laser desorption/ionization mass spectrometric imaging, in vivo reflectance confocal microscopy, echography, and histology: effect of age and peptide applications. *J Cosmet Dermatol* **14**, 152–160.
205 Longuespee R, Ly A, Casadonte R, Schwamborn K, Kazdal D, Zgorzelski C, Bollwein C, Kriegsmann K, Weichert W, Kriegsmann J *et al.* (2019) Identification of MALDI imaging proteolytic peptides using LC-MS/MS-based biomarker discovery data: a proof of concept. *Proteomics Clin Appl* **13**, e1800158.
206 Dunne J, Griner J, Romeo M, Macdonald J, Krieg C, Lim M, Yagnik G, Rothschild KJ, Drake RR, Mehta AS *et al.* (2023) Evaluation of antibody-based single cell imaging techniques coupled to multiplexed imaging of N-glycans and collagen peptides by matrix-assisted laser desorption/ionization mass spectrometry imaging. *Anal Bioanal Chem* **415**, 7011–7024.
207 Drifka CR, Loeffler AG, Mathewson K, Mehta G, Keikhosravi A, Liu Y, Lemancik S, Ricke WA, Weber SM and Kao WJ (2016) Comparison of picrosirius red staining with second harmonic generation imaging for the quantification of clinically relevant collagen fiber features in histopathology samples. *J Histochem Cytochem* **64**, 519–529.

18733468, 2024, 6, Downloaded from https://febs.onlinelibrary.wiley.com/doi/10.1002/1873-3468.14852, Wiley Online Library on [30/08/2025]. See the Terms and Conditions (https://onlinelibrary.wiley.com/terms-and-conditions) on Wiley Online Library for rules of use; OA articles are governed by the applicable Creative Commons License